Appendix A – GSSHA Model Report

Application of the U.S. Army Corps of Engineers' Gridded Surface Subsurface Hydrologic Analysis model to develop groundwater recharge in the Little Rock Creek watershed

James Solstad, Minnesota DNR

The groundwater recharge used by the Little Rock Creek MODFLOW model was computed using the U.S. Army Corps of Engineers' Gridded Surface Subsurface Hydrologic Analysis (GSSHA) model. GSSHA is a physics-based, distributed hydrologic model. The model couples 2-dimensional overland flow and 1-D stream flow with a 2-D single-layer groundwater model. GSSHA can be used as an episodic or continuous model where soil surface moisture, groundwater levels, and stream interactions are continuously simulated. GSSHA was developed by the U.S. Army Corps of Engineers' Engineering Research and Development Center. Additional information regarding the model may be found at
http://www.gsshawiki.com/Gridded_Surface_Subsurface_Hydrologic_Analysis

Model Development

Model Domain: The GSSHA and MODFLOW models have identical model domains (Figure 1). A constant 200m x 200m cell size used was used for the GSSHA model. The model contains 18,987 cells encompassing an area of 293 square miles. Included within the model is the 109 square mile Little Rock Creek watershed.

Topography: A hydrologically-conditioned 3m DEM was used to define the topography for the GSSHA model. The hydrologic-conditioning preserves the stream profile as defined by LIDAR data. Cell elevations were adjusted as needed to eliminate depressions in locations where LIDAR and/or aerial photographs indicate a channel draining that location.

Little Rock Lake was initially modeled as a lake feature using the available bathymetric contours. It was found that removing the lake, i.e., raising cell elevations to just below normal water level, reduced simulation time and reduced mass balance errors.

Stream network: Only the main streams and ditches within the Little Rock Creek watershed were modeled as 1-D channels (Figure A1). The channel profile is based on the hydrologically-conditioned 3m DEM. DNR permit files, bridge plans, and field survey notes were used to help define the channel bottom. Those sources suggest that the channel bottom profile is generally 0.5 - 1m below the 3m LIDAR stream elevation. The entire stream network was initially dropped 1m below the LIDAR profile; calibration results suggested a 0.5m differential provided a better fit for summer baseflow.

The other streams that outlet to the model boundary, including the Platte and Skunk Rivers, were modeled as overland flow. Those flow paths receive water from overland flow and exfiltration from groundwater.

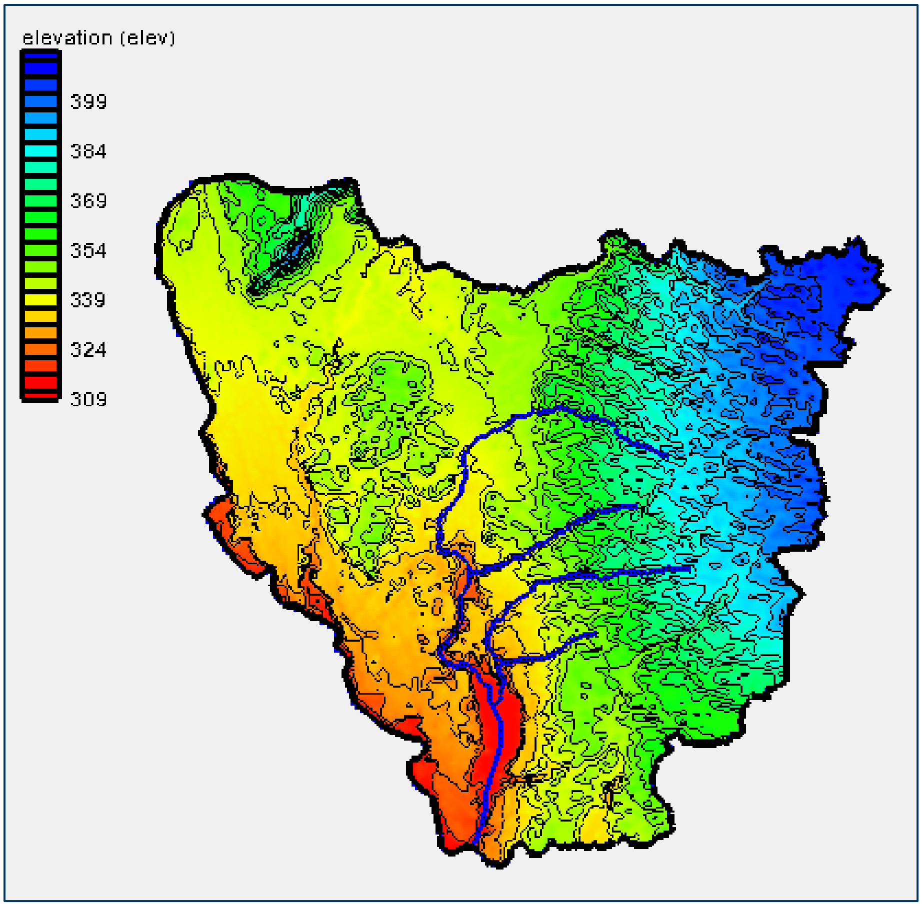

Figure A1: Topography (meters) with the Little Rock Creek watershed 1-D stream network

Land Use: Land use was based on the 2014 version of the U.S. Department of Agriculture Cropland Data Layer. For use in this GSSHA model the numerous classes of this dataset were merged into the following seven categories:

Crops	45%
Alfalfa	16
Small grains	2
Forest	17
Developed	3
Wetland	14
Water	3
	100%

Soils: The Natural Resources Conservation Service Soil Survey Geographic database (SSURGO) was used to define the spatial distribution of the predominant soil map units within the model domain. Within the model domain there are four predominant soil textural classes. Two of those classes were further refined based on their hydrologic soil group, "C" indicating a confining layer within that particular soil map unit. The six textural - hydrologic soil group classifications used in the GSSHA model are shown in Figure A2.

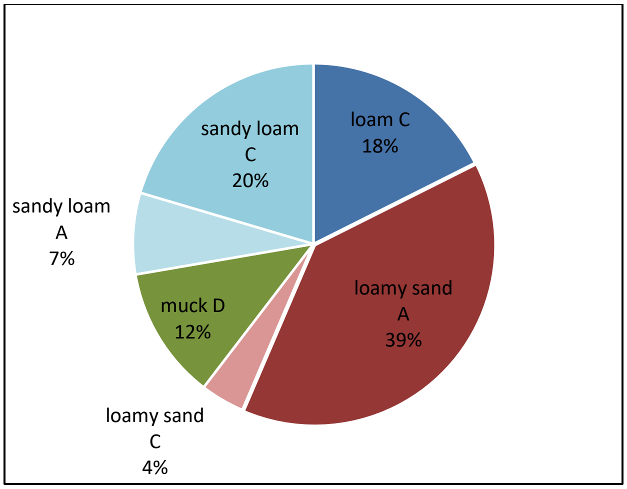

Figure A2: SSURGO textural classes

Geology: The top of bedrock elevation was based on the 30-meter bedrock topography grid developed for the model domain (Figure 6). This dataset defines the depth of the 1-layer groundwater model used by GSSHA. The groundwater index map is based on the Quatrernary geology GIS data layer, as follows:

- Moraine with limited buried aquifers (54%)
- Outwash and terrace with extensive buried aquifers (41%)
- Peat (5%)

Climate: Hourly hydrometeorological data were obtained from the National Climatic Data Center (https://www.ncdc.noaa.gov/). The Little Falls Automated Weather Observing System (AWOS) station was the primary dataset used. Gaps in the Little Falls data were filled using data from the St. Cloud Automated Surface Observing System (ASOS) station. Climate variables include:

- Air temperature
- Barometric pressure
- Wind speed
- Relative humidity
- Percent sky cover

Direct and global radiation are computed by GSSHA.

Precipitation data sources include (Figure A3):

- Daily data (National Weather Service Coop and Minnesota HIDEN) from the MN State Climatology office website (http://www.climate.umn.edu/)
- 20-minute AWOS/ASOS stations (Little Falls and St. Cloud)
- 15-minute tipping buckets rain gages available at selected stream gages

Total storm durations for each precipitation event were obtained from the daily data. Temporal distribution of the precipitation were defined by the 15- and 20-minute data. There was generally good agreement when both the 20-minute AWOS and 15-minute stream gage precipitation data were available; just one high resolution dataset was therefore used for a given event. The daily data were prorated to the selected high resolution source. Events of a few hundredths of an inch were often combined with a larger preceding or subsequent event.

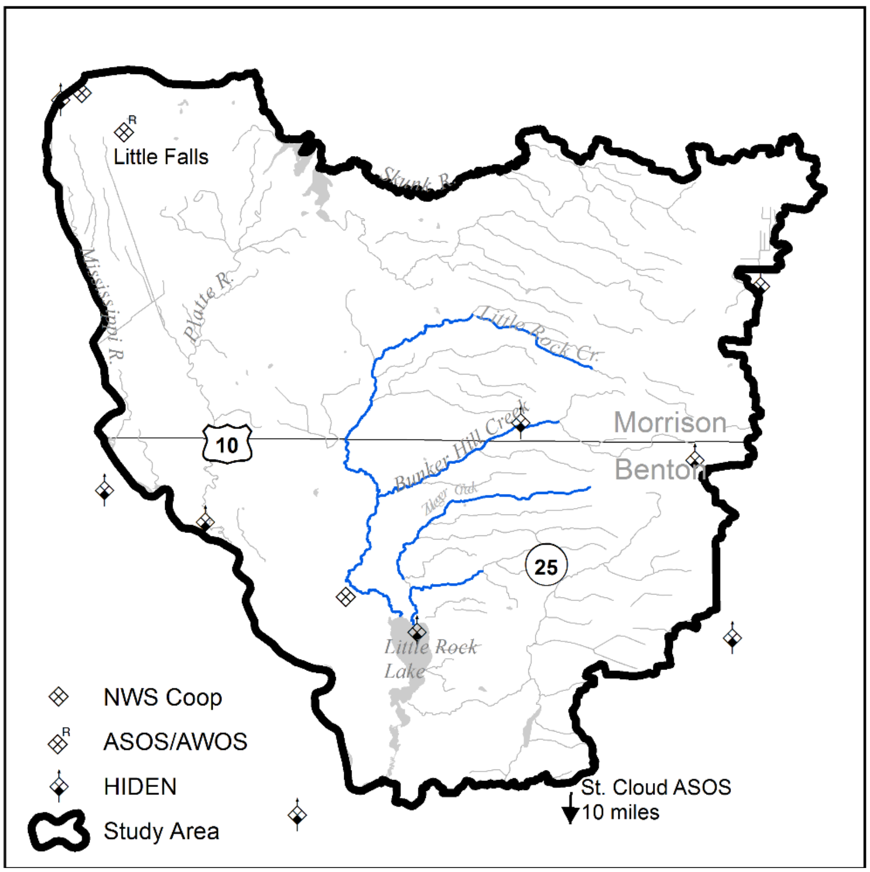

Figure A3: Precipitation stations

Hydrologic processes

Index Maps & Mapping Tables: GSSHA models will contain one or more index maps that describe various aspects of the watershed being modeled, e.g., land use. Each grid cell in a given index map is assigned an integer value corresponding to a unique feature, e.g., forest. A "mapping table" is then used to assign attributes using a selected index map for a given hydrologic process. As an example,

Figure A4 shows a mapping table that is associated with a land use index map to define overland flow roughness.

Roughness							
ID	1	27	36	111	121	141	195
Description1	crops	small grains	alfalfa	water	developed	forest	wetland
Description2							
Surface roughness	0.070000	0.100000	0.100000	0.050000	0.050000	0.250000	0.250000

Figure A4: Mapping table example: surface roughness (Manning's "N") is assigned using a land use index map

Overland flow: GSSHA computes 2-D lateral overland flow (cell to cell) using the diffusive wave equation, a flow routing routine that accounts for backwater conditions. Manning's N is assigned to each cell using the land use index map, as shown in Figure A4. Overland flow routed from adjacent cells, as well as precipitation falling directly on a cell is subject to infiltration.

Channel flow: GSSHA also uses a diffusive wave routine to compute 1-D channel flow. The channel and overbank geometry were defined for each channel reach using data cut from 1m LIDAR. The Manning's N value (a single value for both channel and overbank) was based on visual inspection of aerial photography, as well as fitted during the calibration process. The Manning's N values for this model varied from 0.06 to 0.20.

Infiltration: The 1-layer Green and Ampt with redistribution option in GSSHA was used to simulate infiltration. The infiltration index map was based on a combination of land use and soil texture. Initial soil parameters were assigned using a procedure developed within the DNR that makes use of U.S. Department of Agriculture's SPAW (Soil-Plant-Air-Water) and WEPP (Water Erosion Prediction Project) models. The SPAW model is used to develop the basic Green & Ampt soil parameters for each textural class, including porosity, field capacity, and wilting point. The WEPP provided guidance to define the Green and Ampt effective hydraulic conductivity for each textural class, and the appropriate adjustment for land cover. The hydraulic conductivity was the only infiltration parameter adjusted during calibration.

Evapotranspiration: Potential evapotranspiration (PET) is computed hourly from the hydro-meteorological inputs using the Penman-Monteith method for vegetated soils and a land cover-soils index map. Parameters include land surface albedo, canopy stomatal resistance, vegetation height, and a vegetation transmission coefficient. If the amount of water ponded on the surface does not satisfy the PET demand, actual ET (AET) is based on the amount of soil moisture within the root zone (1m assumed for this model) using an empirically derived equation (Dingman, 1994).

GSSHA includes an option for a global seasonal adjustment for PET by applying a monthly multiplication factor to the stomatal resistance for all land use categories. Since row crops are the predominant land use, maximum evapotranspiration (ET) was set for July and August (a factor of 1). June and September were considered transitional months. The maximum stomatal resistance adjustment factor of four was used for the period October through May.

The computation of ET is a critical component of this analysis, as the amount of groundwater recharge is directly related to ET. The focus during the development of the initial version of this GSSHA model was on getting the overall ET generally correct to calibrate streamflow. The original model version accounted for the additional ET resulting from the water added to the system via irrigation. It did not account for the change in crop yield due to irrigation and its effect on ET and GW recharge.

Additional efforts were taken for this final model version to: 1) correctly compute the relative amounts of ET among the various land use categories; and 2) account for the change in ET due to the increased crop productivity associated with irrigation.

As GSSHA does not have a plant growth routine, the Water Erosion Prediction Project (WEPP) model was used to estimate crop growth and associated ET volumes for the various land use conditions. WEPP was developed by the USDA's Forest Service, Agricultural Research Service, and Natural Resources Conservation Service and the U.S. Department of the Interior's Bureau of Land Management.

WEPP is a continuous simulation model that can use site specific data. For this study, two sets of runs were computed using two of the predominant soil texture classes, loamy sand and loam. St. Cloud climate and daily precipitation data were used, as well as the sequence of irrigation used in the GSSHA model.

WEPP includes numerous "management schemes" for varying land uses. Five management schemes were chosen to correspond to the land use categories of the GSSHA model. There are numerous crop management schemes; several test runs did not find a significant difference in the computed annual ET between, say, "corn, soybean-spring chisel plow", and "corn, soybean, mulch tillage." Once the basic soil and climate data are entered into the program, it's an easy task to complete numerous iterations of varying management and irrigation scenarios. Key results are shown in Figure A5.

A small (192 cells) GSSHA model was used to develop relationships between stomatal resistance and computed ET for the same loamy sand and loam soils used in the WEPP model. This model was run numerous times with varying vegetation height and stomatal resistance values using the same climate data as the larger GSSHA model, and essentially the same as the WEPP model. The net result of these runs are a set of curves relating the key PET parameter (stomatal resistance) with the computed average annual ET; the curves for loamy sand soils are shown in Figure A6. Figure A7 highlights the nearly linear relationship between ET and groundwater recharge.

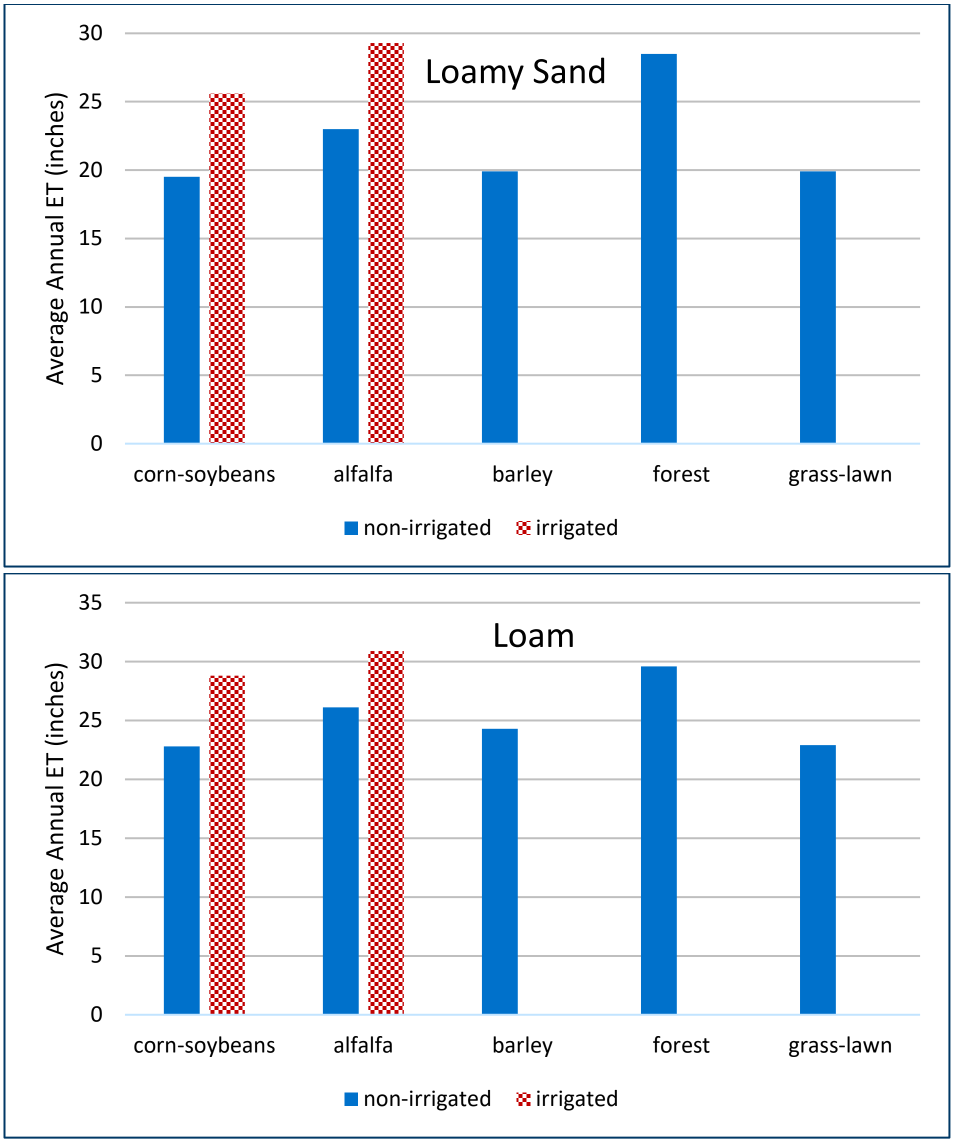

Figure A5: Average Annual ET computed by the WEPP model (10-year simulation: 2005-2014)

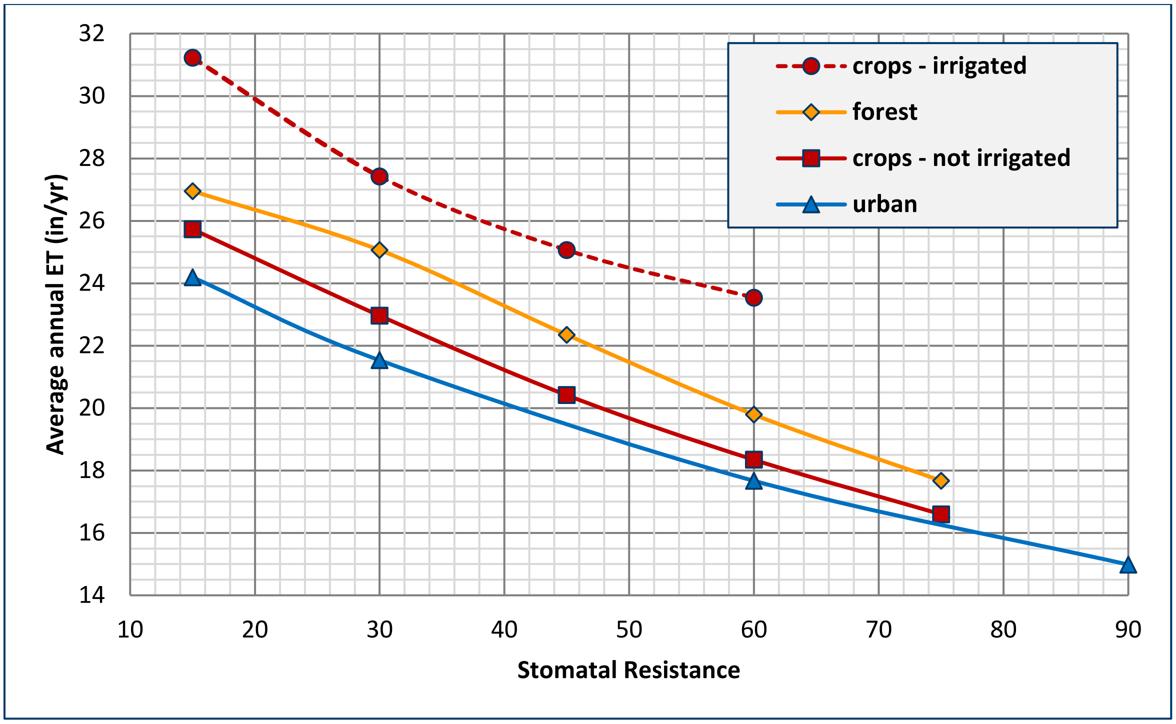

Figure A6: GSSHA computed relationships between stomatal resistance and average annual ET for a loamy sand. These relationships are based on a series of model simulations using uniform soil and land cover and the same 10-year simulation period as used with the WEPP model.

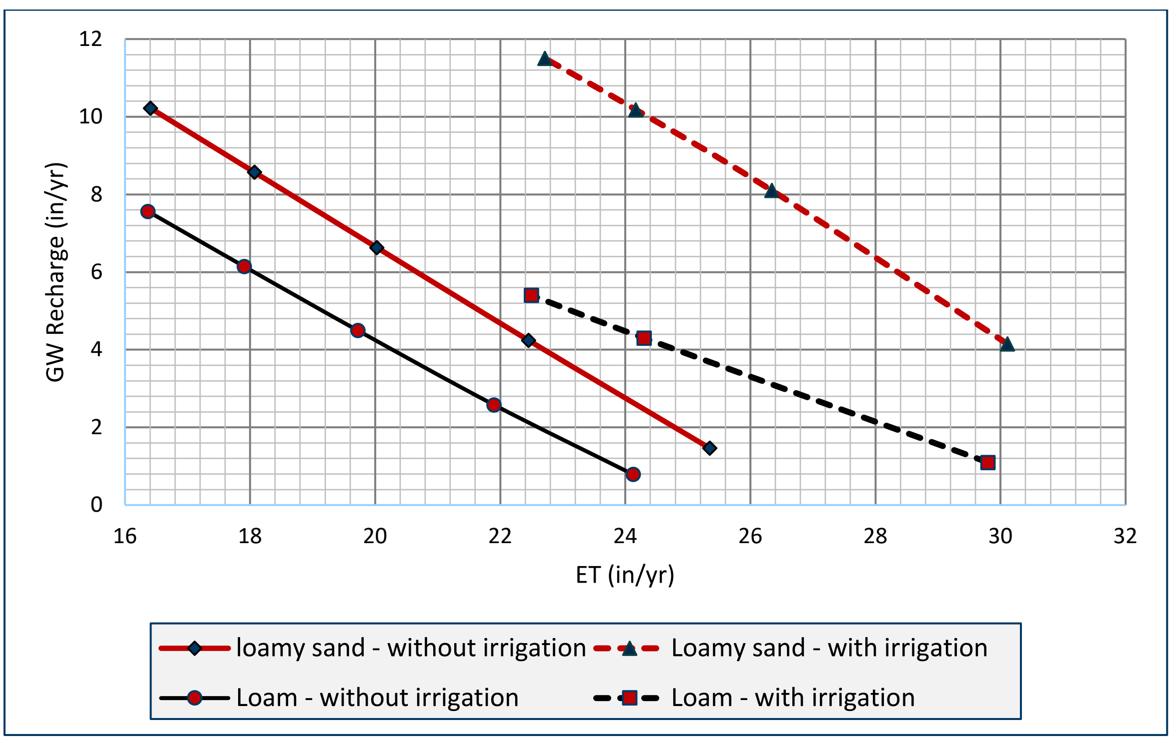

Figure A7: GSSHA developed relationships between average annual ET and groundwater recharge

The appropriate stomatal resistance for a given land use-soil combination were determined using the WEPP-computed ET for a given land cover (Figure A5) with the relationships in Figure A6. As an example, the WEPP computed average annual ET for irrigated crops is 25.6 inches (Figure A5); the corresponding stomatal resistance (dashed red line in Figure A6) is 41.

The computed flows were too low when using the WEPP-derived stomatal resistance values in the large GSSHA model, indicating the computed ET was too high. A series of subsequent runs found that multiplying all baseline stomatal resistance factors by 1.7 produced acceptable results.

Groundwater flow: A lateral 2-d simulation of saturated groundwater flow is included in the model. Stream losses and gains to and from the water table are governed by a river flux boundary condition. Groundwater may also exfiltrate (discharge to the surface) if the water table rises above the land surface. Exfiltrated water may be stored at the surface, re-infiltrate, or be routed as overland flow depending on the depth of water in a cell. The following two parameters are incorporated into the model using the geology index map:

	Hydraulic Conductivity (cm/hr)	Porosity
Moraine	4	0.28
Outwash terrace	32	0.30
Peat	1	0.25

Snow accumulation and melt: GSSHA includes three methods to simulate snow accumulation and melt: Energy Balance, Temperature Index, and a Hybrid Energy Balance. The energy balance method was found to best simulate the timing of snowmelt runoff in the Little Rock Creek watershed.

GSSHA also includes a Continuous Frozen Ground Index (CFGI) option for use during long-term simulations. Infiltration ceases when the index is below a user specified threshold. That threshold was found to vary widely from year to year. Each water year was run separately using a fitted CFGI threshold for that year.

Groundwater appropriation & irrigation: GSSHA's spatially explicit nature allows wells and irrigated fields to be added on a cell-by-cell basis. Each well is assigned to a specific cell within the GSSHA model; a volume of water is removed from the groundwater at that location based on a supplied time series for that particular well. Similarly, irrigated water is added back into the model as an overland boundary condition. Several cells were typically identified for each irrigation permit based on examination of aerial photographs and permit files. A time series file was also used to specify the timing and amount of irrigated water added to the system. The location of the wells and irrigated cells is shown in Figure A8.

The GSSHA model adds irrigated water directly to the land surface, i.e., the model does not simulate any plant interception of the irrigated water. The irrigated volume was therefore set to 92% of the pumped volume to produce a reasonable net irrigation efficiency allowing for drift, droplet evaporation, and wetted canopy (interception) evaporation losses. Once the irrigated water is added to a given cell, it is treated the same as precipitation, i.e., available for surface ponding, runoff, infiltration, and evapotranspiration.

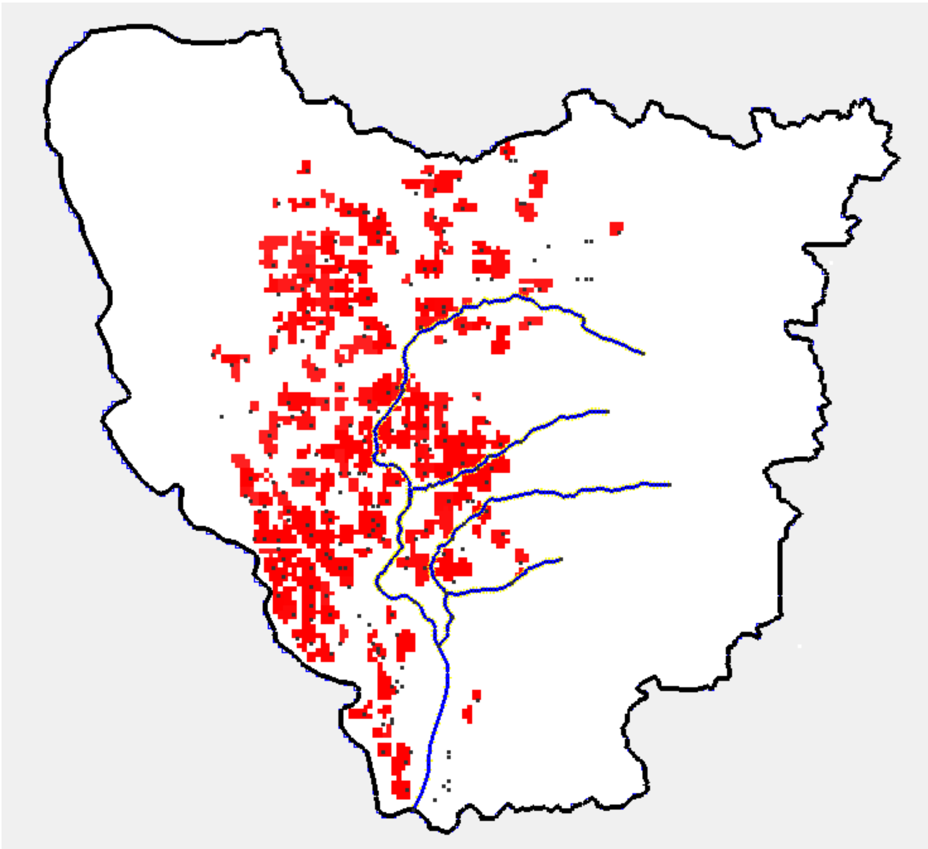

Figure A8: Groundwater appropriation (wells indicated by black points) and irrigated cells (red cells)

Calibration Procedure

Stream Gages: Three stream gages on Little Rock Creek operated by the DNR and MPCA were used during calibration (15029001, 15029005, and 15031001) as well as available stream flow measurements on Bunker Hill Creek (15028001 and 15028002):

Observation Wells: Numerous observation wells are located within the model domain. The computed water table was checked at four observation wells (5004, 49002, 49028, and 49034) to gain an additional sense of model performance.

Simulation period: The GSSHA model was run for a 10-year period (October 2004 through September 2014), one water year (October through September) at a time. The computed water table, soil moisture, and overland water depths at the end of one year were used as a "hotstart" for the subsequent year. The first two years are considered a warm-up period; the summary statistics that follow are therefore provided for Water Years 2007 through 2014.

General approach: An initial set of parameters was based on guidance in the GSSHA wiki, as well as previously developed GSSHA models for Dobbins Creek in Mower County and Shakopee Creek in Kandiyohi County. The initial set of runs focused on snowmelt, followed by a sequential progression of other key parameters. Fine-tuning of parameters was based on visual comparison of the plotted hydrographs, and computation of annual volumes and the Nash-Sutcliffe efficiency coefficient. An automated calibration routine was not used due to the long run times (approximately 7 hours for a 1-year simulation).

Key calibration parameters include:

- Green & Ampt effective hydraulic conductivity
- Stomatal Resistance
- Groundwater hydraulic conductivity
- Stream Manning's N and near channel hydraulic conductivity

Scenarios

Two scenarios were run in additional to existing conditions:

1. No groundwater withdrawal, no irrigation, no change in land use - The stomatal resistance values for irrigated crops were adjusted to reflect the lower anticipated ET (red to blue bars in Figure A5, and the corresponding stomatal resistance values from Figure A6 multiplied by the factor 1.7 as explained above)
2. No groundwater withdrawal, no irrigation, irrigated crops changed to non-irrigated alfalfa

Results

Various aspects of the simulation results are displayed in Figures A9 through A19; summary water budget numbers are included on the last page.

This GSSHA model does a reasonably good job of simulating key hydrologic processes within the Little Rock Creek watershed. An average Nash-Sutcliffe efficiency coefficient of 0.62 and 0.72 was obtained for gage stations 15029001 and 15031001, respectively.

The focus during calibration was on obtaining a good match between computed results and observed data for summer base flow. This was generally achieved most years. However, the computed storm-event flows were often low, especially during extended periods of wetter climatic conditions (e.g., September 2010 and August 2011). As a result, the overall computed discharge is 13% and 26% below the comparable measured flow at gages 15029001 and 15031001, respectively. As the summer and fall computed base flow are generally acceptable suggests that computed ET that is higher than actual ET may be compensating for the likely higher computed infiltration volumes.

The overall computed ET for Scenario 2 is slightly higher than the results for existing conditions (page A-20). As expected, the computed water table for the existing conditions (w/ pumping) is lower for cells near the wells. The additional amount of ET due to irrigation is in part being offset by the reduction of transpiration from the water table. In addition, these results are showing less "direct evaporation" for the pumping scenario (page 20), i.e., evaporation of ponded water on the land surface.

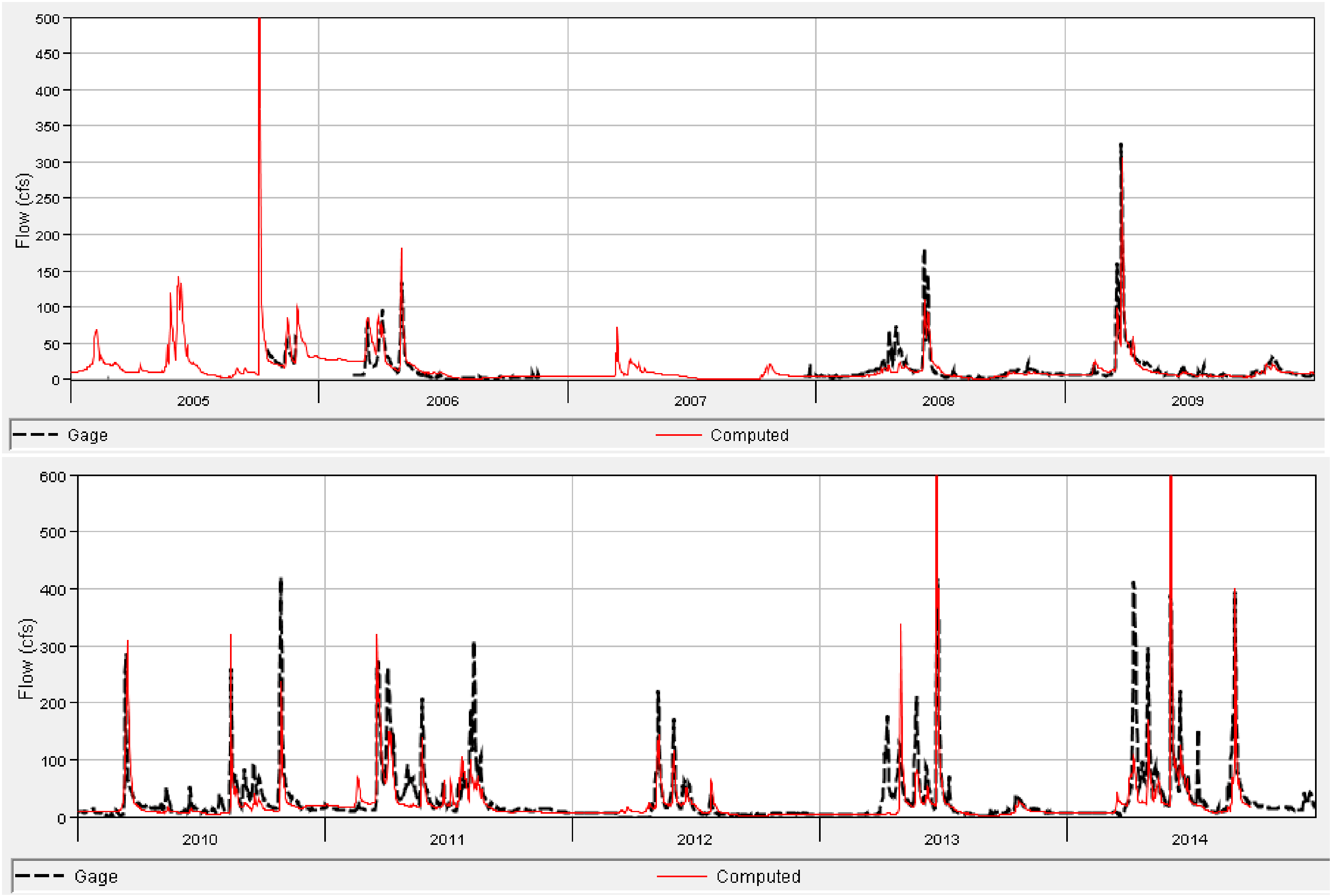

Figure A9: Measured and computed flows at Little Rock Creek gage station 15029001

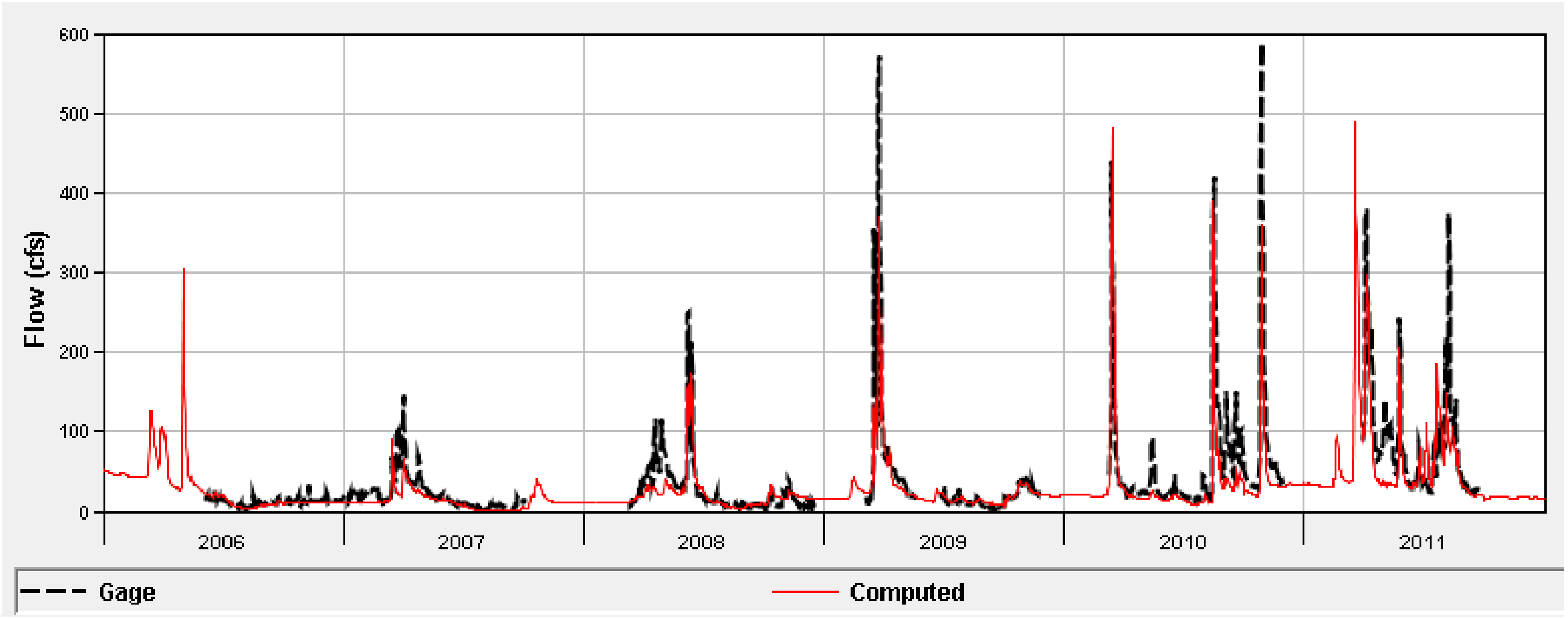

Figure A10: Measured and computed flows at Little Rock Creek gage station 15031001

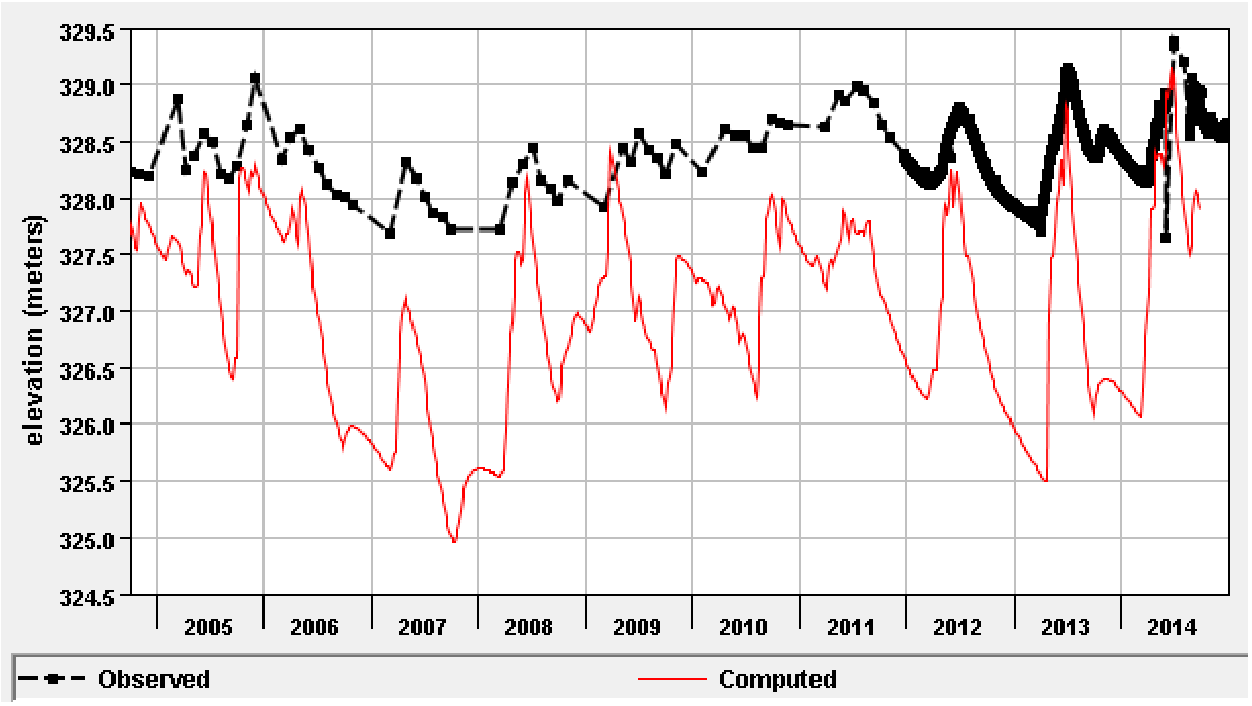

Figure A11: Measured and computed water table elevations @ Obwell 5004

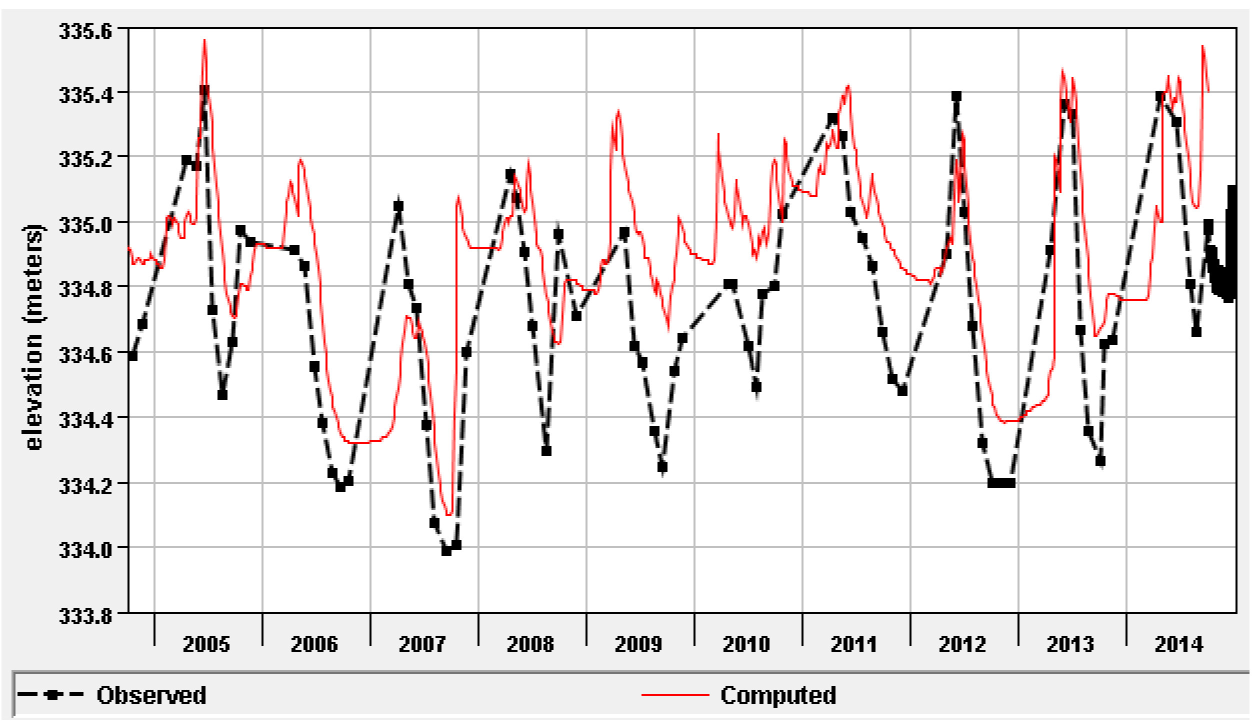

Figure A12: Measured and computed water table elevations @ Obwell 49002

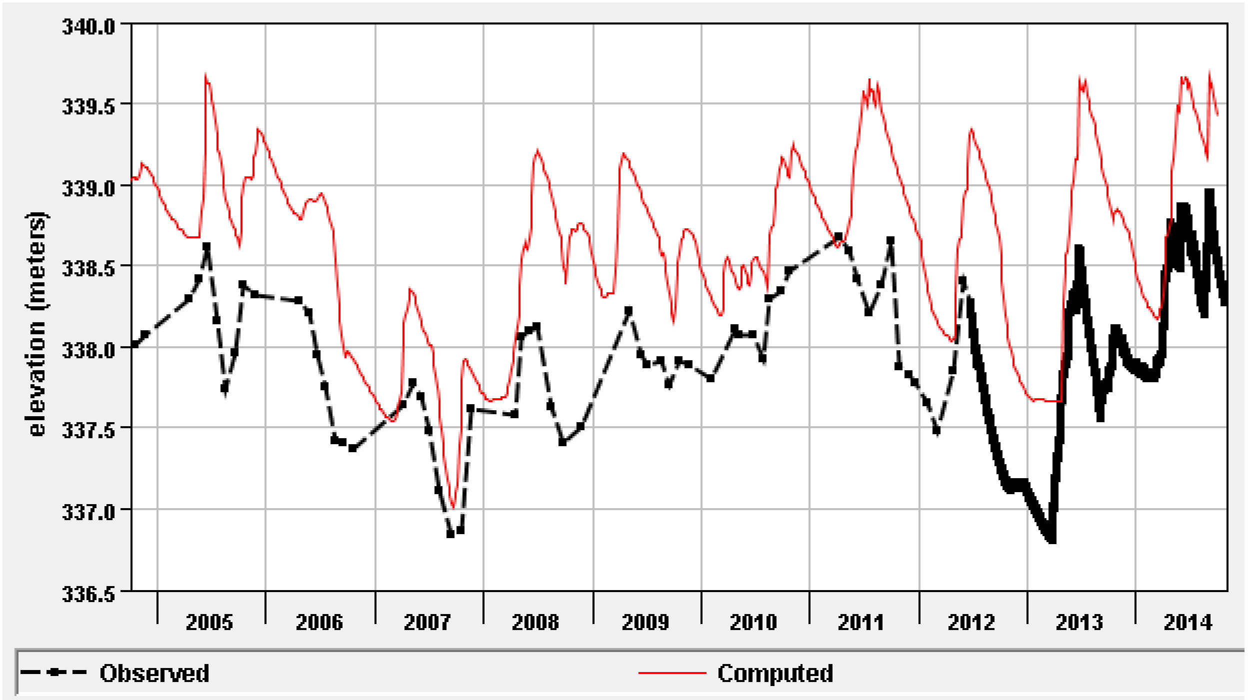

Figure A13: Measured and computed water table elevations @ Obwell 49028

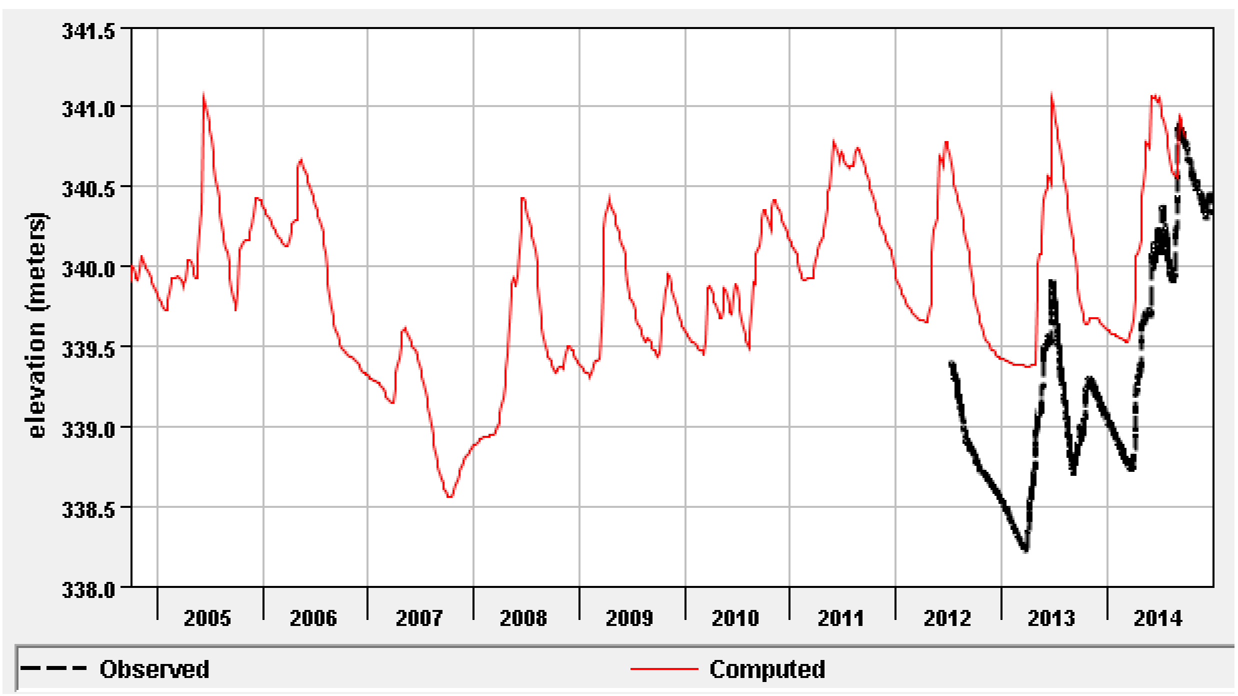

Figure A14: Measured and computed water table elevations @ Obwell 49034

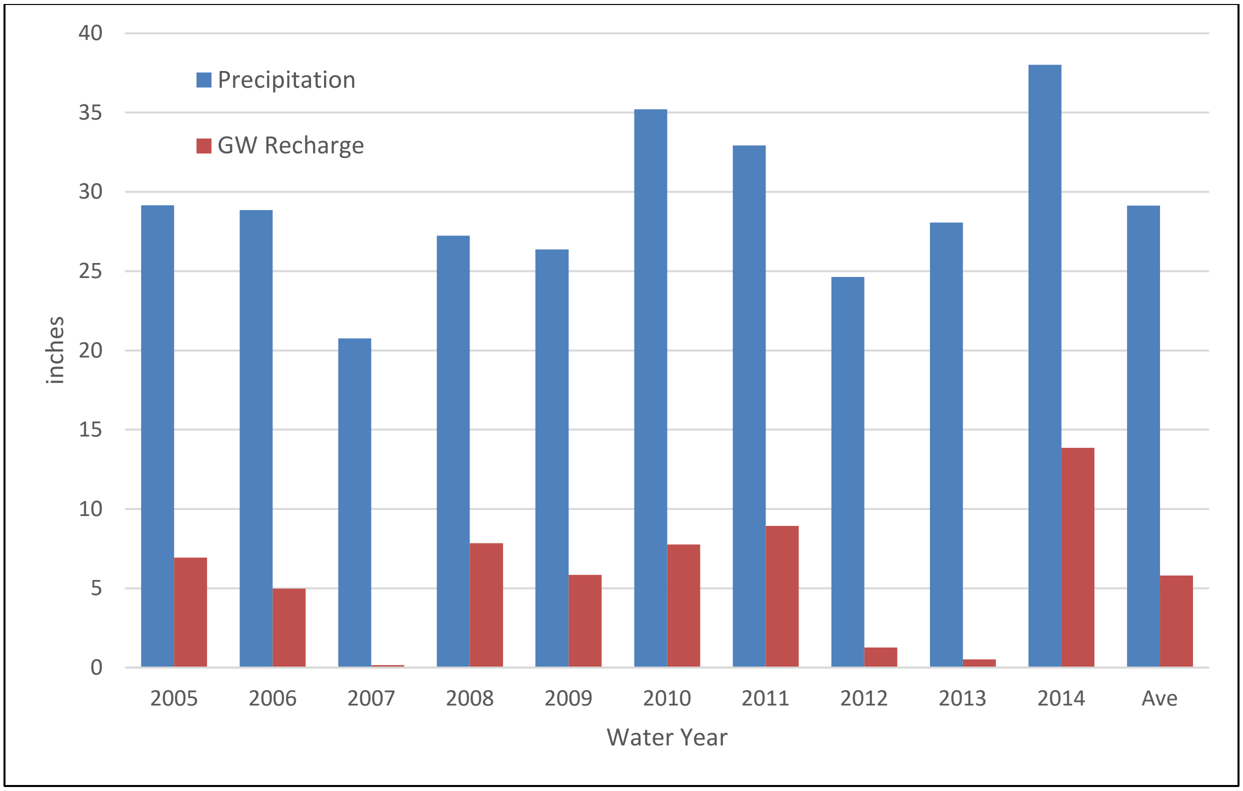

Figure A15: Annual precipitation and computed groundwater recharge, average over the model domain

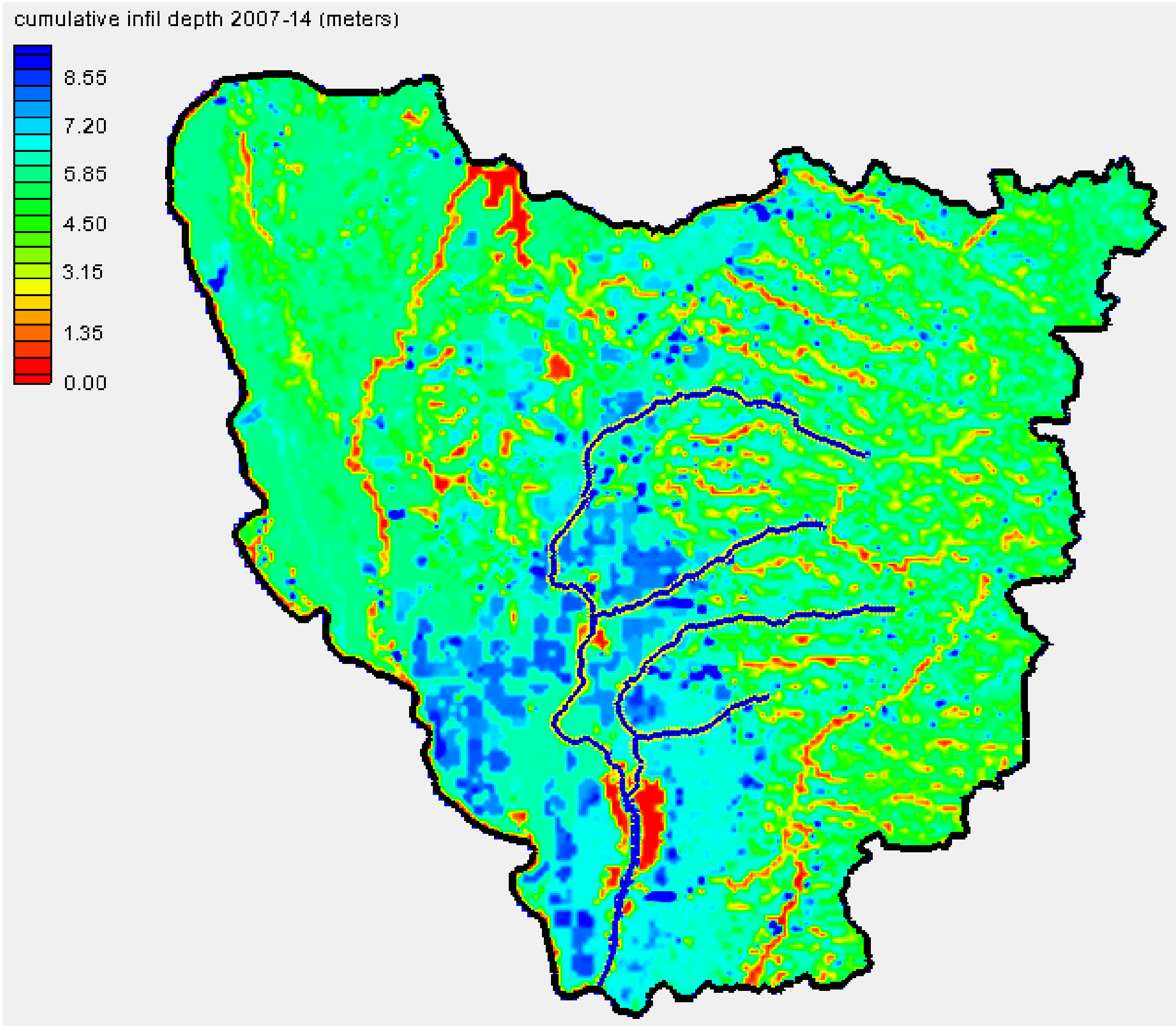

Figure A16: Cumulative infiltration depth (meters), water years 2007 through 2014. (The color ramp was chosen to highlight the key differences; the cumulative infiltration depth in a small number of grid cells exceed the range shown on this figure.)

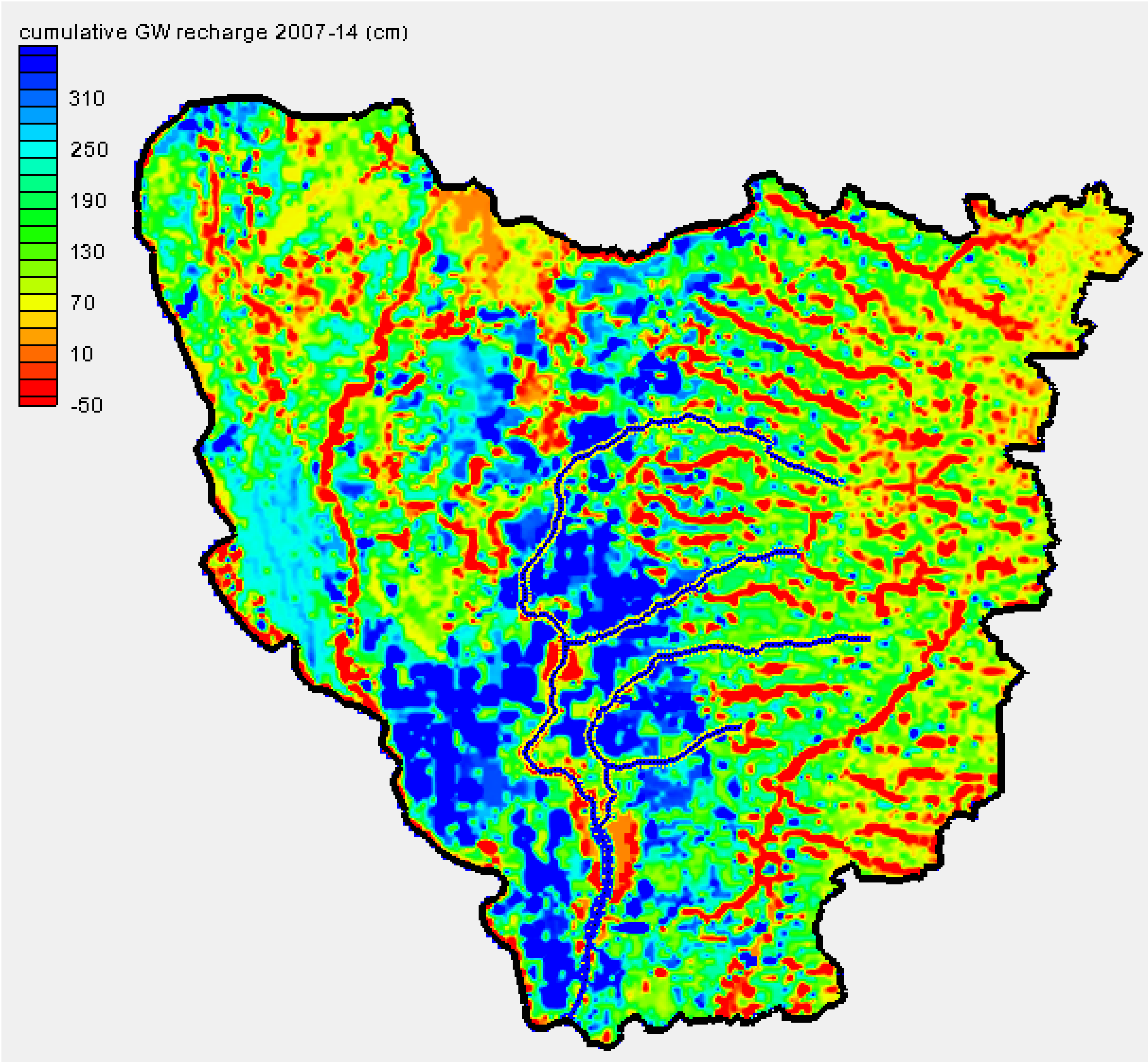

Figure A17: Cumulative groundwater recharge (cm), water years 2007 through 2014. (The color ramp was chosen to highlight the key differences; the recharge depth in a small number of grid cells exceed the range shown on this figure.)

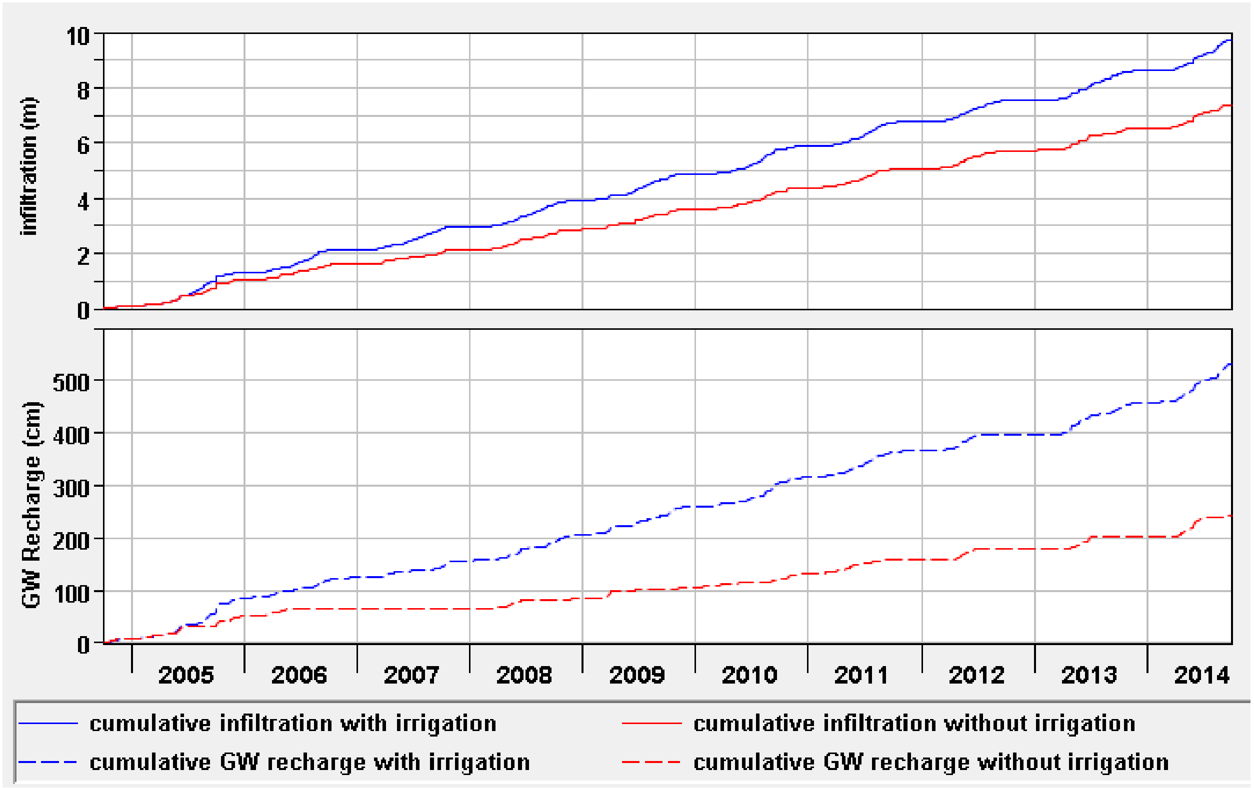

Figure A18: Cumulative infiltration and groundwater recharge at a representative cell (60:86) - comparing with and without irrigation scenario 2.

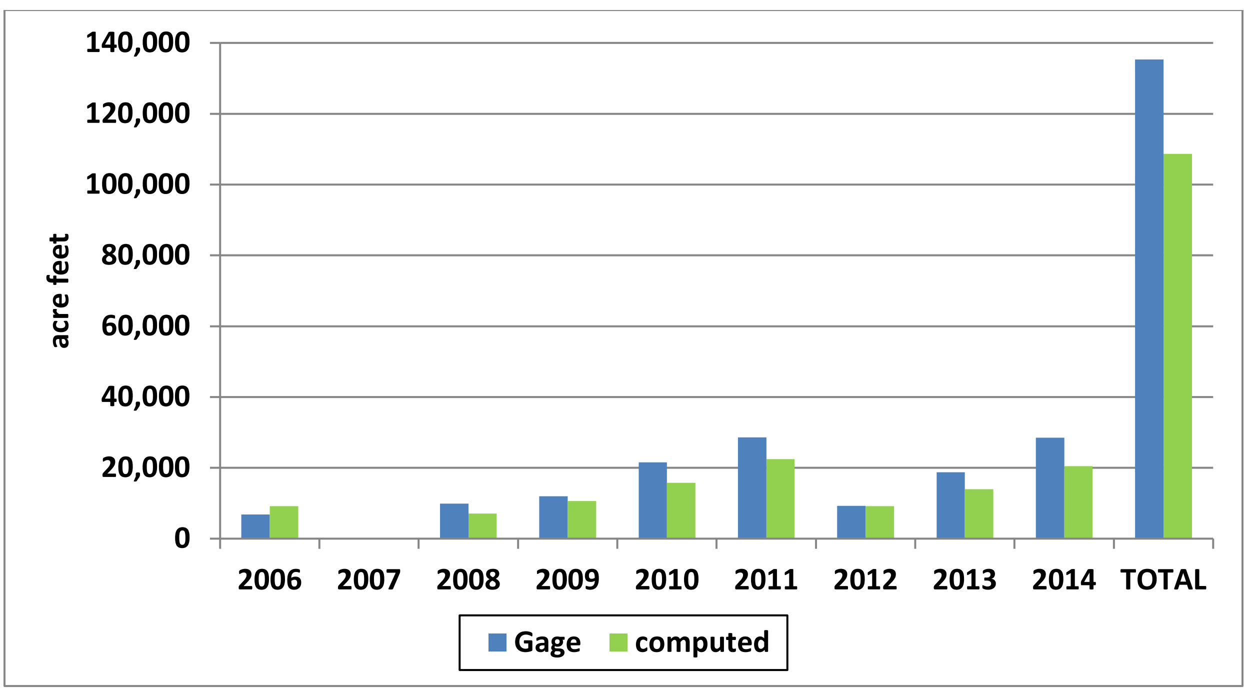

Figure A19: Comparison of measured vs. computed flow volume at Gage 15029001

Overall model water budget summary - water years 2007 through 2014 (inches):

	Existing	Scenario1	Scenario2
Precipitation	233.2	233.2	233.2
Infiltration	199.8	192.6	193.6
Total ET	191.5	191.2	193.4
Direct Evap	37.1	39.4	37.6
Exfiltration[1]	29.3	32.2	29.9
Recharge to GW[2]	50.9	45.9	42.8
Total Pumped from GW	6.8	0.0	0.0
Volume lost to boundary	19.6	20.8	20.0
Irrigation Volume[3]	5.9	0.0	0.0
Lateral Inflow to channels	11.7	12.5	11.8
Total Q (LRC outlet)	23.6	25.3	23.8
Stream channels to GW	4.0	4.0	4.0
GW to stream channels	15.9	16.8	16.1
Precipitation+Irrigation-ET-Pump-Vol Lost-Total Q	-2.3	-4.1	-3.9
Net Change in Volume	4.4	4.4	4.4
Mass balance error (in)	6.7	8.5	8.3
% of Precipitation	2.9%	3.6%	3.6%

[1] Exfiltration is discharge of groundwater (GW) to the land surface

[2] Recharge to groundwater is net recharge that includes negative values when and where groundwater moves into to the soil zone and is ultimately transpired.

[3] The irrigation volume applied to the soil surface is 92% of the irrigation pumping volume. The difference between total pumped from GW and irrigation volume includes pumping for uses other than crop irrigation and assumed irrigation losses of 8% not accounted for through model processes.

References

Abraha, Michael, et al., 2015, Evapotranspiration of annual and perennial biofuel crops in a variable climate: *GCB Bioenergy*, 7(6), 1344-1356. https://doi.org/10.1111/gcbb.12239

Dingman, S. Lawrence, 2002, *Physical Hydrology*, 2nd Edition: Waveland Press, Inc.

Hamilton S.K., 2015, Comparative water use by maize, perennial crops, restored prairie, and poplar trees in the US Midwest: *Environmental Research Letters*, 10 064015. http://iopscience.iop.org/article/10.1088/1748-9326/10/6/064015/meta

Saxton, Keith E., U.S. Department of Agriculture Agricultural Research Service and the Department of Biological Systems Engineering, and Washington State University, *Soil – Plant – Air – Water Field & Pond Hydrology*, Version 6.02.75.

U.S. Department of Agriculture-Agriculture Research Service, National Soil Erosion Research Lab, and Purdue University, WEPP Hillslope/Watershed Model, Version 2012.800, August 2012.

Wagle, et al., 2017, Analysis and estimation of tallgrass prairie evapotranspiration in the central United States: Agricultural and Forest Meteorology 232 (2017)

Appendix B – Base-Flow Analysis, Paired Watershed, and Climate Summary Reports

Baseflow Analysis in Little Rock Creek

December 22, 2020

Little Rock Creek is a designated trout stream located in central Minnesota (Figure 1). Its streamflow is sustained during dry periods under baseflow conditions. It flows perennially, remaining open during the winter, indicating a strong connection between groundwater and surface water with inputs from wetlands and lakes, seepage from the stream banks, upper soil profile, and groundwater inflow from connected aquifers. The August median baseflow was calculated at the long term gage H15029001 located near Rice MN. August median baseflow is used as an index because it represents typical flows and can be used as an indicator of aquatic habitat under typical low flow conditions.

Baseflow Calculation Method and Results

Little Rock Creek stream gaging station H15029001 located near the City of Rice, MN, has a period of record beginning in 1998 that is intermittent until 2008 and then continuous through 2020, with the exception of some missing data in July-December of 2015 due to equipment issue. In order to get estimates of daily baseflow in August of 2015, the streamflow record was estimated using the upstream gaging station: H15029003, Little Rock Creek nr Rice, CSAH26 by plotting the daily values at H15029001 and H15029003, fitting a regression, and then using the equation to estimate the missing values at H15029001.

Using this measured daily streamflow record, the Web-based Hydrograph Analysis Tool (WHAT) model developed by Purdue University (Eckhardt, 2005) was used to estimate the daily baseflow values. This method is available online and is widely accepted for baseflow separation. Using the record of daily estimated baseflow, the median of all available August daily baseflow values was calculated for the time periods that correspond to the DNR Little Rock Creek Area hydrological model (Table 1).

Simulated baseflow time period	August median baseflow (cfs)
2006 and 2008 through 2012	4.6
2006 and 2008 through 2018	6.8

Table 1: The above table lists August median baseflow at station H15029001 calculated using the WHAT (Web-based Hydrograph Analysis Tool)- Purdue University for DNR MODFLOW modeled time periods.

Figure 2 shows the NOAA Palmer Drought Severity Index (PDSI) for Minnesota Climate Division 5 for each August from 2006 through 2018. The PSDI uses precipitation and temperature data to estimate relative dryness or wetness. Much of the record falls in the mid-range category, however 2016 to 2018 fall into the moderate to very moist categories. As the length of the continuous stream flow record increases at this site the August Median baseflow will be less affected by more extreme years. The record at H15029001 is a moderate length to conduct statistical analysis.

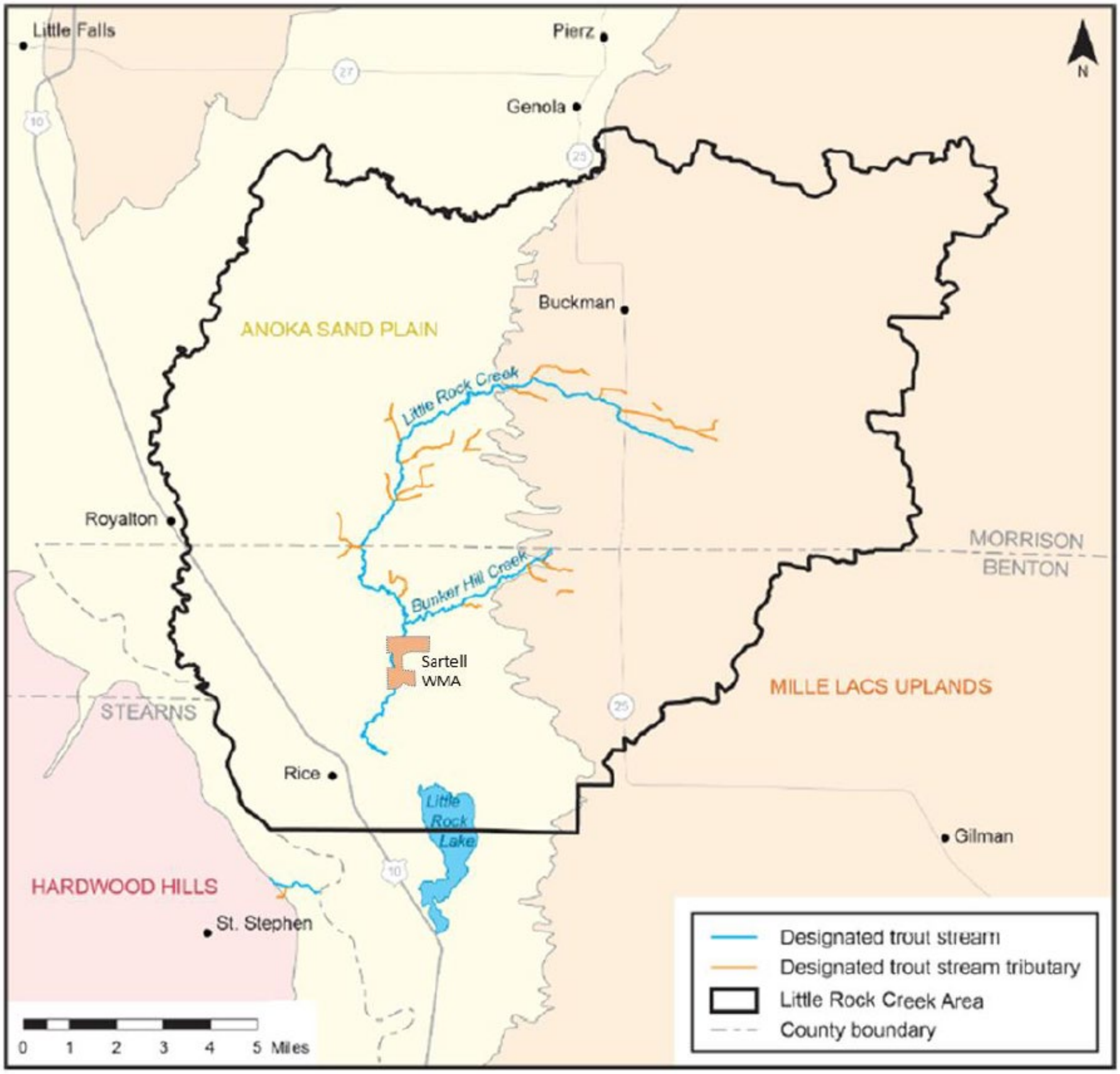

Figure 1. This figure shows the Little Rock Creek Area.

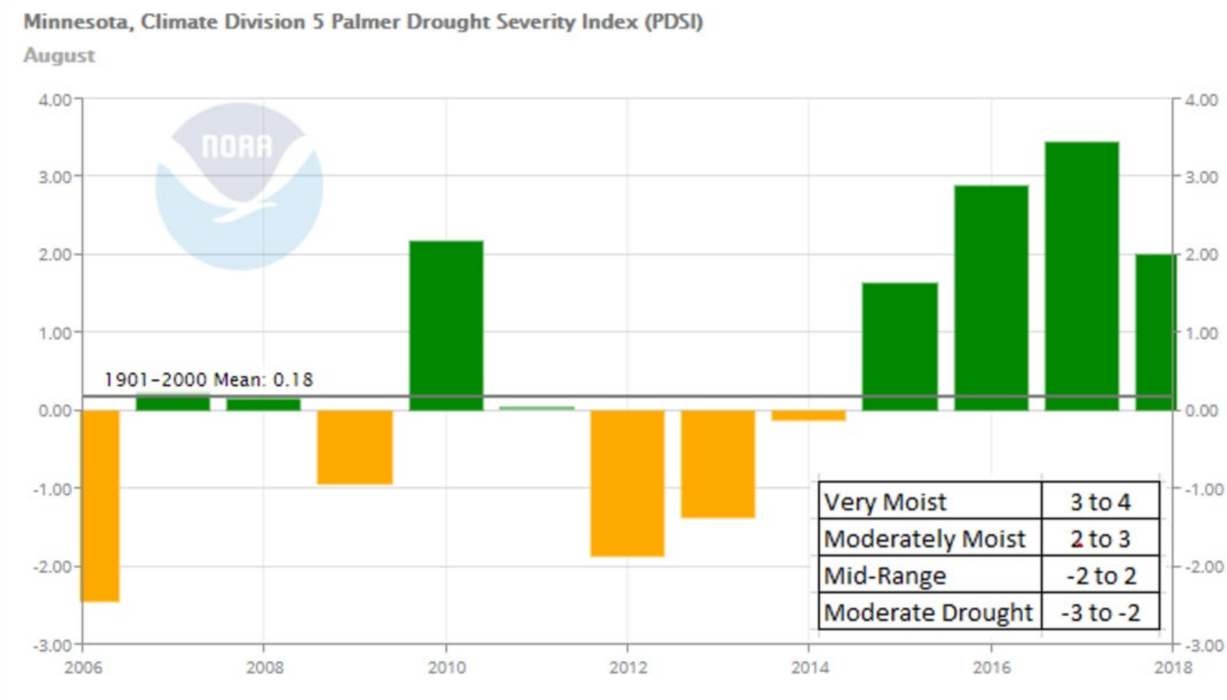

Figure 2. This chart shows the NOAA Palmer Drought Severity Index for Climate Division 5 (Central Minnesota) for the month of August from 2006 to 2018.

References

Eckhardt, K., 2005, How to construct recursive digital filters for baseflow separation: Hydrol. Process., 19: 507–515. doi:10.1002/hyp.5675

NOAA National Centers for Environmental information, Climate at a Glance: Divisional Time Series, published November 2020, retrieved on November 27, 2020 from https://www.ncdc.noaa.gov/cag/

Comparing Baseflow in Little Rock Creek and Rice Creek Watersheds

December 30, 2020

Little Rock Creek is located in central MN in an area of concentrated groundwater use (Figure 1). The Minnesota Department of Natural Resources initiated studies in 2015 to determine if groundwater use was sustainable in the area. Pumping can reduce the natural cycle of groundwater discharge to streams (baseflow) which may negatively impact the ecosystem. Stream baseflow reduction can be used as an indicator for this impact.

Paired watershed studies are widely used to evaluate effects of water management practices on hydrology. This method uses two watersheds to study different water management scenarios. The watersheds need to be similar in land use, landscape characteristics, and assumes there is a consistent and predictable relationship between response variables (Clausen and Spooner, 1993). This study was completed to determine if baseflow differences exist between two similar watersheds with different groundwater-use rates.

The USGS tool StreamStats (US Geological Survey, 2016) was used to find a comparable watershed to Little Rock Creek. Rice Creek watershed is similar to Little Rock Creek watershed (Table 1). It is located approximately 25 miles southeast of Little Rock Creek and is of a similar size and characteristics however it has substantially less permitted groundwater use. Modeled baseflow calculated using measured streamflow in each watershed was compared to determine if there were differences in baseflow.

Model Development

Paired watershed: Rice Creek and Little Rock Creek watersheds have many similarities indicated by StreamStats (Table 1). A stream gage exists on Rice Creek at the lower end of the watershed near the City of Clear Lake (gaging station 17038001) and the Little Rock Creek's lower end gage station is near Rice (H15029001, Figure 1). There is a correlation between Rice Creek and Little Rock Creek's daily discharge values. With an r-squared value of 0.69, it can be stated that Rice Creek's flows can explain roughly 70% of flow recorded at Little Rock Creek (Figure 2). Unlike Rice Creek, Little Rock Creek is heavily irrigated. The baseflow model will be validated by comparing modeled and observed flows in Rice Creek then running different water management scenarios in Little Rock Creek.

Comparison Methods: Baseflow values were computed at the Rice Creek gage (17038001) and the Little Rock Creek gage (15029001) using the Web-based Hydrograph Analysis Tool (WHAT) model developed by Purdue University (Eckhardt, 2005). These computed baseflow values were then normalized for watershed area creating baseflow per square mile. Normalization eliminates the effects of slightly different drainage areas of the two watersheds, which allows for a more consistent comparison. Normalization, or the watershed area ratio is a common technique for estimating streamflow of two similar watersheds (Archfield and Vogel, 2010). The summers of 2008 and 2009 were selected for this analysis because these were normal to dry years when streamflow was less influenced by excessive runoff. The Palmer Hydrological Drought Index indicates July and August of 2008 and 2009 were considered midrange for general hydrologic conditions (Table 2). Additional years of record were considered but not used because of above-normal precipitation and/or incomplete streamflow records.

Model Results

The normalized baseflow hydrographs for 2008 and 2009 have a similar shape and trend, which indicates that the two watersheds respond similarly during summer baseflow conditions (Figures 3 and 4). The Rice Creek watershed has substantially less reported groundwater use than the Little Rock Creek watershed (Table 3). For example in 2008 and 2009, the groundwater use in the Rice Creek watershed was 9-34% of the appropriation in the Little Rock Creek watershed (Table 3).

The modeled August 2008 and 2009 baseflow values for Rice Creek and Little Rock Creek were compared to the DNR Little Rock Creek Area MODFLOW modeled difference of 'current use' and 'no-use' scenarios (in both cubic feet per second (cfs) and normalized cubic feet per second (cfs/mi^2, Table 4). In summary, several conclusions from this paired watershed study.

- Rice Creek and Little Rock Creek have similar watershed characteristics including size, land use, soil types and groundwater resources (Table 1).
- In 2008 and 2009, groundwater appropriation in the Rice Creek watershed ranged between 9% and 34% of the reported groundwater appropriation in the Little Rock Creek watershed (Table 3).
- Normalized baseflow for Rice Creek for August 2008 and 2009 was 59% and 26% greater than the baseflow of Little Rock Creek (Table 4, Figure 3 and 4).
- MODFLOW 'current use' versus 'no-use' simulated baseflow for Little Rock Creek for August 2008 was 59% and August 2009 was 16% greater without appropriations (Table 4).
- The watershed comparison of physical properties and use provide validation of the DNR Liitle Rock Creek Area MODFLOW model's ability to reasonably simulate the watershed, appropriations, and groundwater flow contributions to Little Rock Creek.

In summary, this paired watershed study indicates that Rice Creek and Little Rock Creek are similar and can be used to test the reasonableness of model outputs developed for the Little Rock Creek Area.

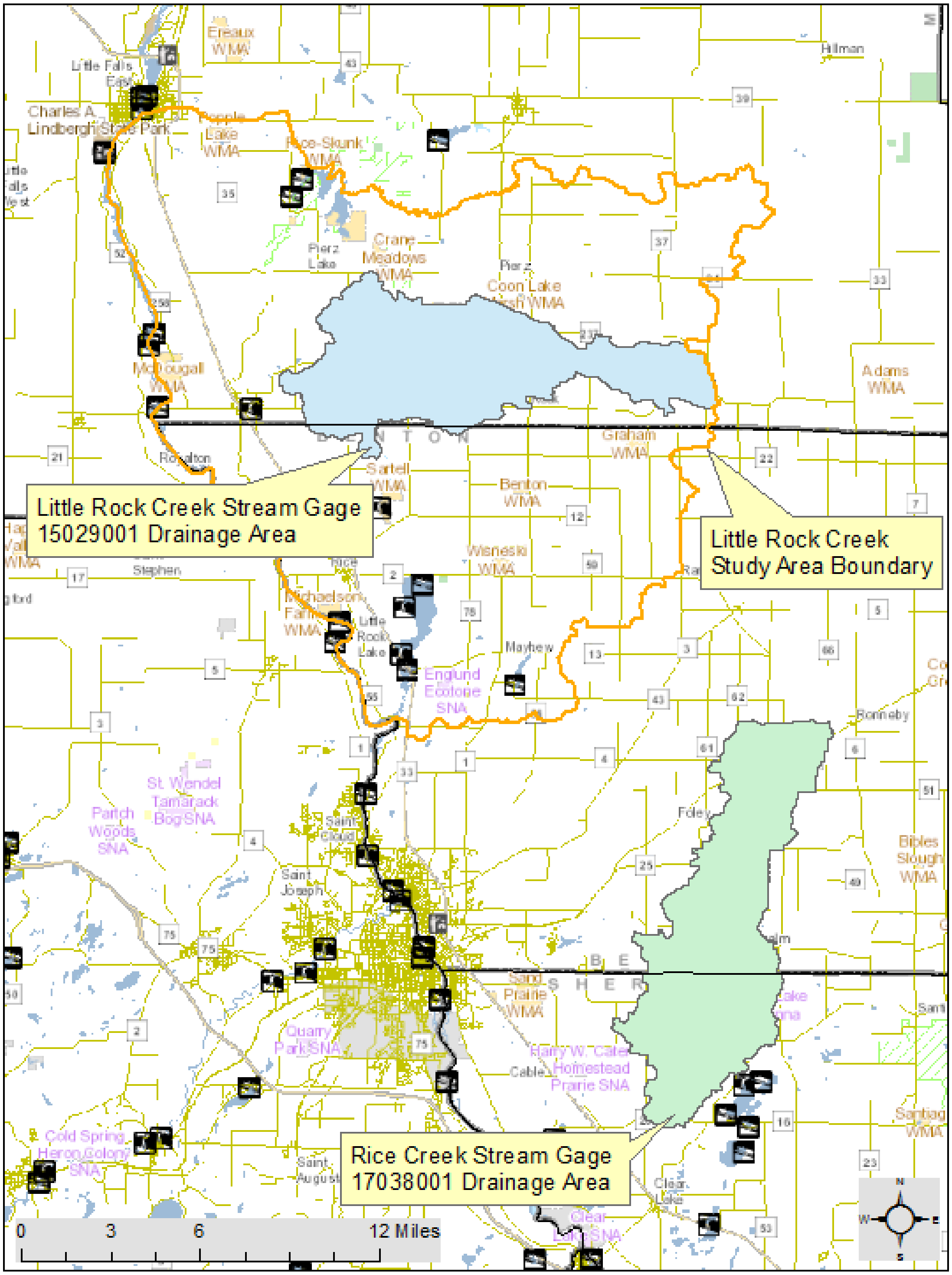

Figure 1: This figure shows the Rice Creek watershed in relation to the Little Rock Creek watershed and the larger Little Rock Creek study area.

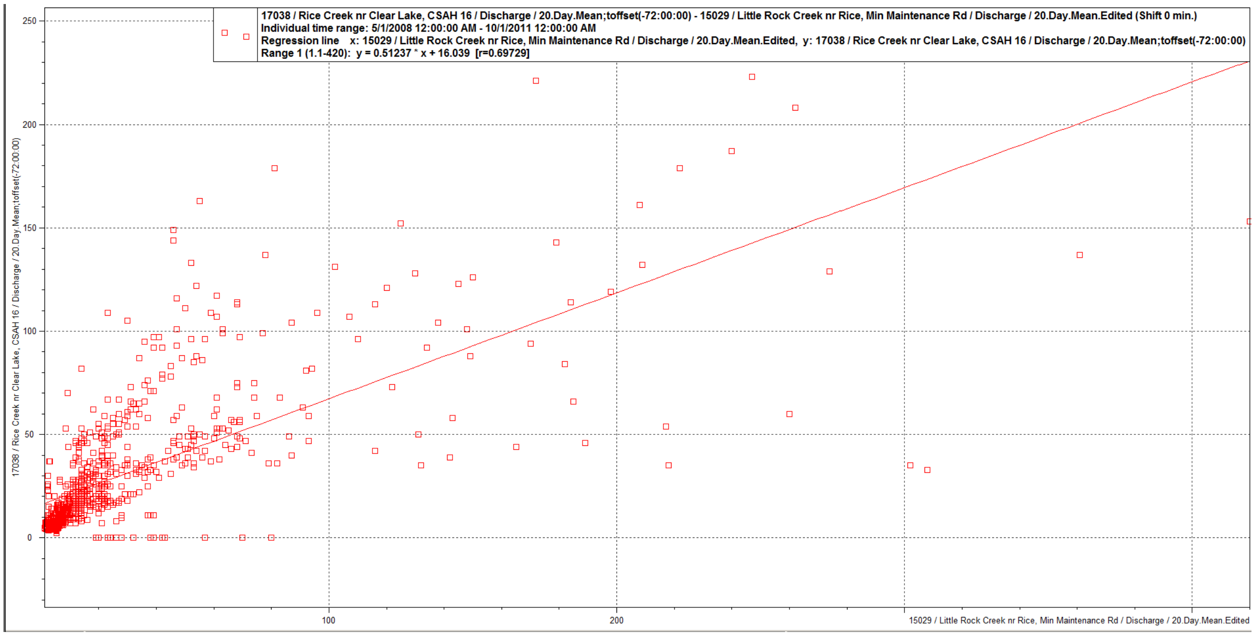

Figure 2: This figure shows the plotted daily discharge values for the Rice Creek and Little Rock Creek data from 2008 year to 2011. The regression yielded an R^2 value of 0.69.

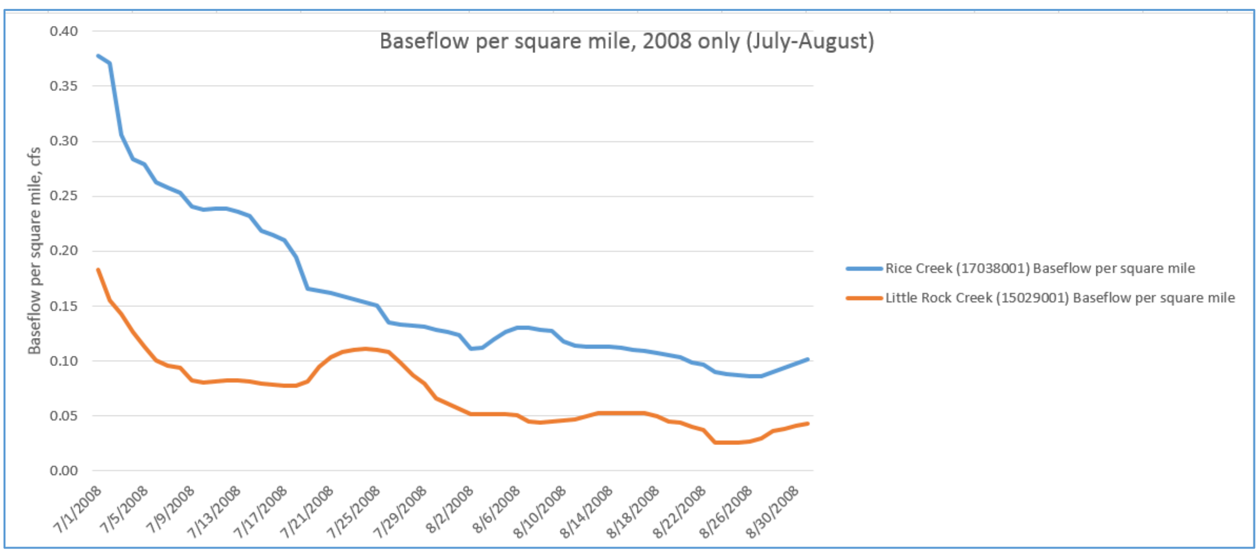

Figure 3: This figure shows the modeled baseflow hydrographs of Little Rock Creek and Rice Creek during summer 2008.

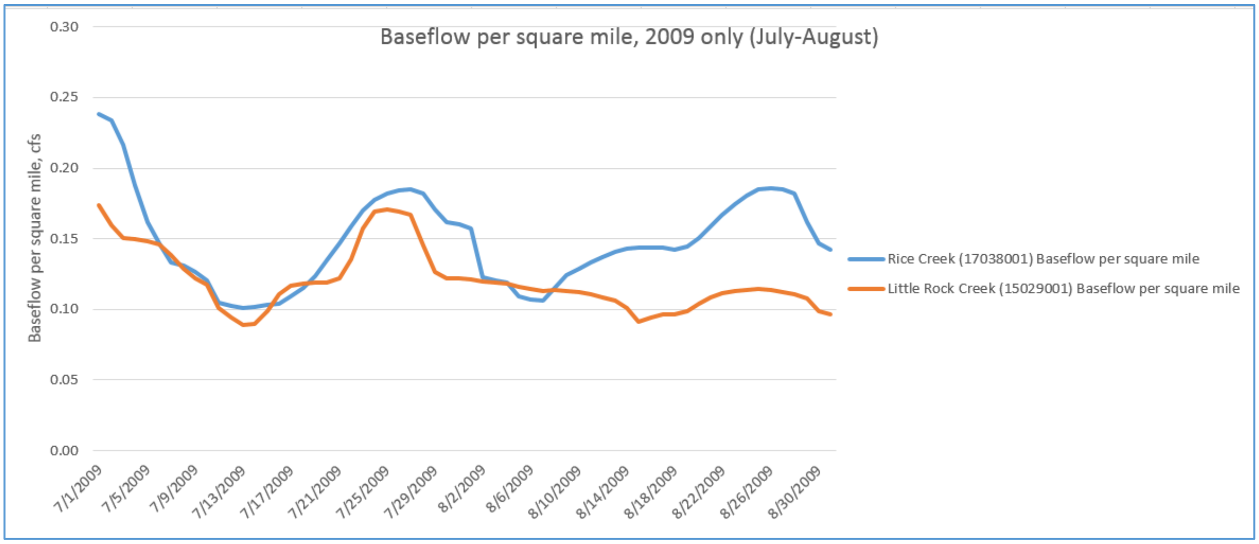

Figure 4: This figure shows the modeled baseflow hydrographs of Little Rock Creek and Rice Creek during summer 2009.

StreamStats Output Report				
	Rice Creek near Clear Lake		Little Rock Creek near Rice	
Latitude	45.48667		45.80963	
Longitude	-93.9798		-94.19729	
Parameters				
Name	Value	Unit	Value	Unit
Drainage Area	45.74	square miles	42.82	square miles
Lakes and Ponds	0.52	percent	0	percent
Storage (NWI water bodies and wetlands)	19.5	percent	22	percent
Hydrologic Soil Type A	34.2	percent	31.5	percent
Hydrologic Soil Type C	33.6	percent	42.7	percent
Organic Matter in Soils	6.52	percent	2.08	percent
Cultivated Crops	68.7	percent	74.6	percent
Forest	13.7	percent	7.59	percent
Developed (Urban) Land	0.0664	percent	0.0335	percent
Impervious Area	1.87	percent	0.53	percent
Mean Annual Runoff	5.51	inches	5.92	inches
Logarithm base 10 of Drainage Area	1.66	Log base 10	1.63	Log base 10
Mean Basin Slope	2.01	percent	1.67	percent

Table 1: The table above lists the values determined from StreamStats for the Little Rock Creek watershed to the nearby Rice Creek watershed.

	Monthly Palmer Hydrological Drought Index					
			Year			
	2006	2007	2008	2009	2010	2011
June	1.26	-2.23	0.79	-1.57	0.59	4.16
July	-2.48	-3.42	0.66	-1.71	1.19	5.09
August	-2.47	-2.82	0.15	-0.96	2.16	4.59
September	-1.78	-2.22	0.23	-1.65	3.87	3.29
		Moderately Moist		2 to 3		
		Mid-Range		-2 to 2		
		Moderate Drought		-2 to -3		
		Severe Drought		-3 to -4		
		Extreme Drought		-4+		

Table 2: The table above shows the monthly Palmer Hydrological Drought Index values 2006 through 2011.

	Rice Creek Watershed Appropriation (Mgal)	Little Rock Creek Watershed Appropriation (Mgal)	Rice Creek percentage of Little Rock Creek
2008			
June	71	344	21%
July	229	792	29%
August	243	811	30%
September	79	359	22%
2009			
June	110	350	31%
July	267	786	34%
August	111	801	14%
September	31	341	9%

Table 3: The table above lists the total groundwater use in the Rice Creek and Little Rock Creek watersheds, obtained from the MNDNR Permitting and Reporting System (MPARS). Gallons listed are the amounts reported by permitted water users.

	August 2008 cfs	August 2008 cfs/mi²	August 2009 cfs	August 2009 cfs/mi²
Little Rock Creek monthly baseflow	1.88	0.044	4.62	0.108
Rice Creek monthly baseflow	4.94	0.108	6.63	0.145
Difference	3.06	0.064	2.01	0.037
Difference (%)	62%	59%	30%	26%
MODFLOW 'current use' monthly baseflow, 15029001	1.16	0.027	3.94	0.092
MODFLOW 'no-use' monthly baseflow, 15029001	2.78	0.065	4.71	0.110
Difference	1.62	0.038	0.77	0.018
Difference (%)	58%	59%	16%	16%

Table 4: The table above compares the August median baseflow of the Little Rock Creek and Rice Creek watersheds, and the difference of the modeled 'current use' and 'no-use' baseflow scenarios.

References

Archfield, S.A., Vogel, R.M., 2010. Map correlation method: selection of a reference streamgage to estimate streamflow at ungaged catchments. WaterResour. Res. 46, W10513

Barlow, P.M., Cunningham, W.L., Zhai, Tong, and Gray, Mark, 2014, U.S. Geological Survey Groundwater Toolbox, a graphical and mapping interface for analysis of hydrologic data (version 1.0): User guide for estimation of base flow, runoff, and groundwater recharge from streamflow data: U.S. Geological Survey Techniques and Methods, book 3, chap. B10, 27 p., http://dx.doi.org/10.3133/tm3B10.

Barlow, P.M., Cunningham, W.L., Zhai, Tong, and Gray, Mark, 2016, U.S. Geological Survey Groundwater Toolbox version 1.2.0, a graphical and mapping interface for analysis of hydrologic data: U.S. Geological Survey Software Release, 01 October 2016, http://dx.doi.org/10.5066/F7R78C9G

Eckhardt, K., 2005, How to construct recursive digital filters for baseflow separation: Hydrol. Process., 19: 507–515. doi:10.1002/hyp.5675

J. C. Clausen and J. Spooner, "Paired Watershed Study Design," Office of Wetlands, Oceans and Watersheds, Environmental Protection Agency, Washington DC, 1993

"Welcome to Streamstats!" *USGS.gov* United States Geological Survey, 21 Feb. 2017, accessed 23 Jan. 2017 at URL https://water.usgs.gov/osw/streamstats/index.html

"WHAT: Web-based Hydrograph Analysis Tool" *Purdue.edu* Purdue University, accessed 12 Jan. 2017 at URL https://engineering.purdue.edu/~what/

Mississippi River - Sartell Watershed Climate Summary

Including the Little Rock Creek Area

December 28, 2020

Kenneth Blumenfeld

Senior Climatologist, Minnesota Department of Natural Resources

Minnesota's climate is changing rapidly, and more changes are coming. In the past several decades, our state has seen increased precipitation, heavier downpours, substantial warming during winter and at night, but also more snow. Little Rock Creek is north and west of the City of Rice, MN and is in the Mississippi River – Sartell watershed. In the 2010s alone, the Little Rock Creek area saw four of its ten warmest years, four of its ten wettest years, and three of its snowiest winters on record—with those records spanning at least 125 years. The 2010s finished as the wettest, snowiest, and second warmest on record.

Little Rock Creek Area Climate

Precipitation in the Little Rock Creek area increased by an average of four inches between 1970 and 2019. Heavy precipitation became more frequent and more intense as well. Daily precipitation totals of at least one inch are 15-30% more common and the typical heaviest rainfall of the year are 10-15% larger than during the middle of the 20th century. Seasonal snowfall totals have increased to historical high marks during this time, despite sharp warming during winter. Three of St. Cloud's ten snowiest winters on record occurred during the 2010s.

The Little Rock Creek area has warmed by an average of over 2.5 degrees F since 1970. This warming has been observed in every season, but is most pronounced at night, and during winter. For the period 1970 through summer of 2020, average daily low temperatures increased more than twice as fast as average daily high temperatures. Winter temperatures increased about six times faster than summer temperatures. So while the average summer high temperature (June through August) increased by just three-tenths of a degree Fahrenheit, a typical winter low temperature increased by over six degrees F. Heat extremes have not yet increased in any part of Minnesota., The highest temperatures of summer and the frequency of 90-degree F days remains well within historical ranges, even as overall temperatures have risen.

More climatic changes on the way for Minnesota

The Mississippi River – Sartell watershed is located in the middle of the continent, half-way between the equator and the North Pole. The region is highly sensitive to large-scale climatic changes and since 1970 has warmed 40% faster than the global average. Global temperature increases are expected to continue and virtually all climate model scenarios project that Minnesota will get much warmer in the decades ahead, including during the summer. Heat extremes will become more common by the middle of this century. The same climate models project more precipitation, more days with heavy precipitation, and greater precipitation extremes. Minnesota and the region will continue to have a highly variable climate. This means that even as we see warmer and wetter conditions, we will still have some cool years, some dry years, and even some significant drought, which is likely to be amplified by continued warming.

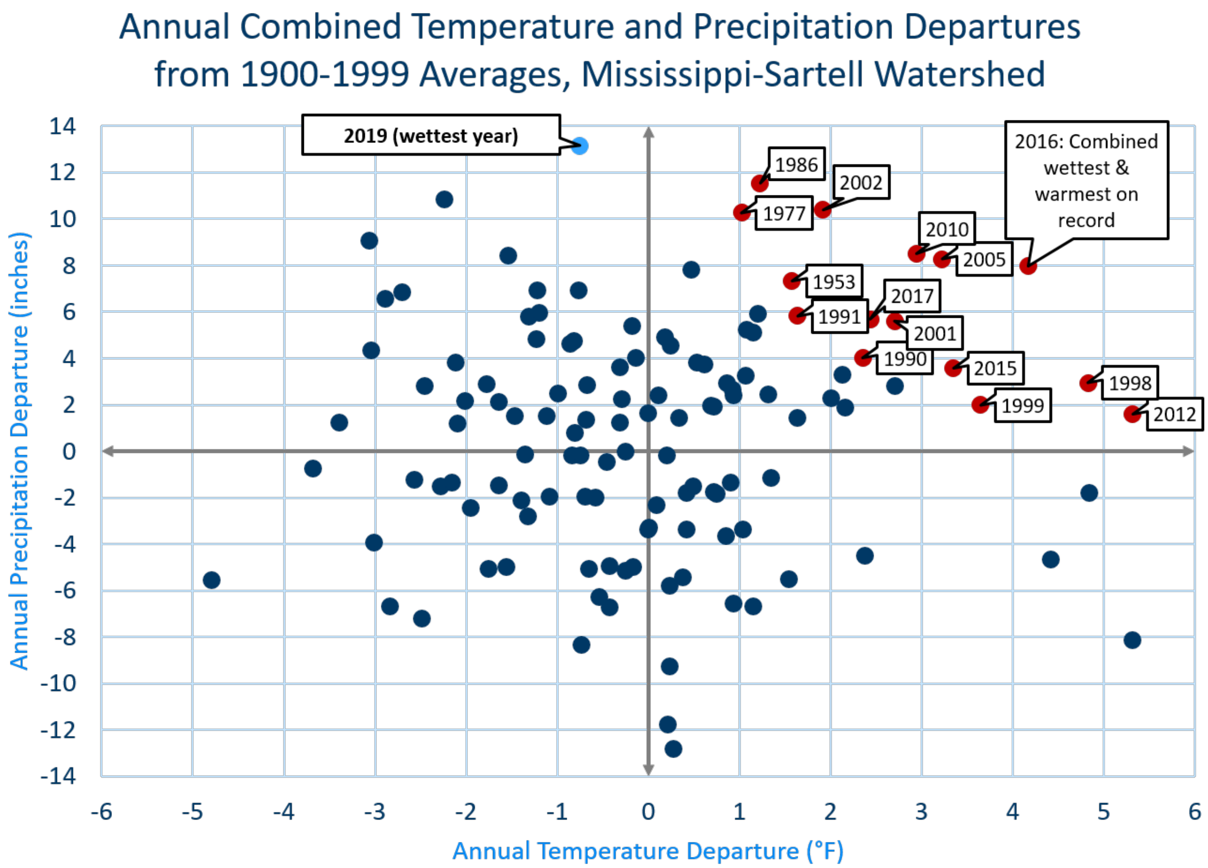

Figure 6

The figure above shows annual precipitation, 1895-2019, in the Mississippi-Sartell Watershed. Wettest year (in 2019) called out. Note that since 1895 the annual precipitation increased over a half-inch per decade. The trend since 1970 (not shown above), is even greater; + 0.80 inches per decade. Data from DNR Climate Trends Tool (https://arcgis.dnr.state.mn.us/ewr/climatetrends/#).

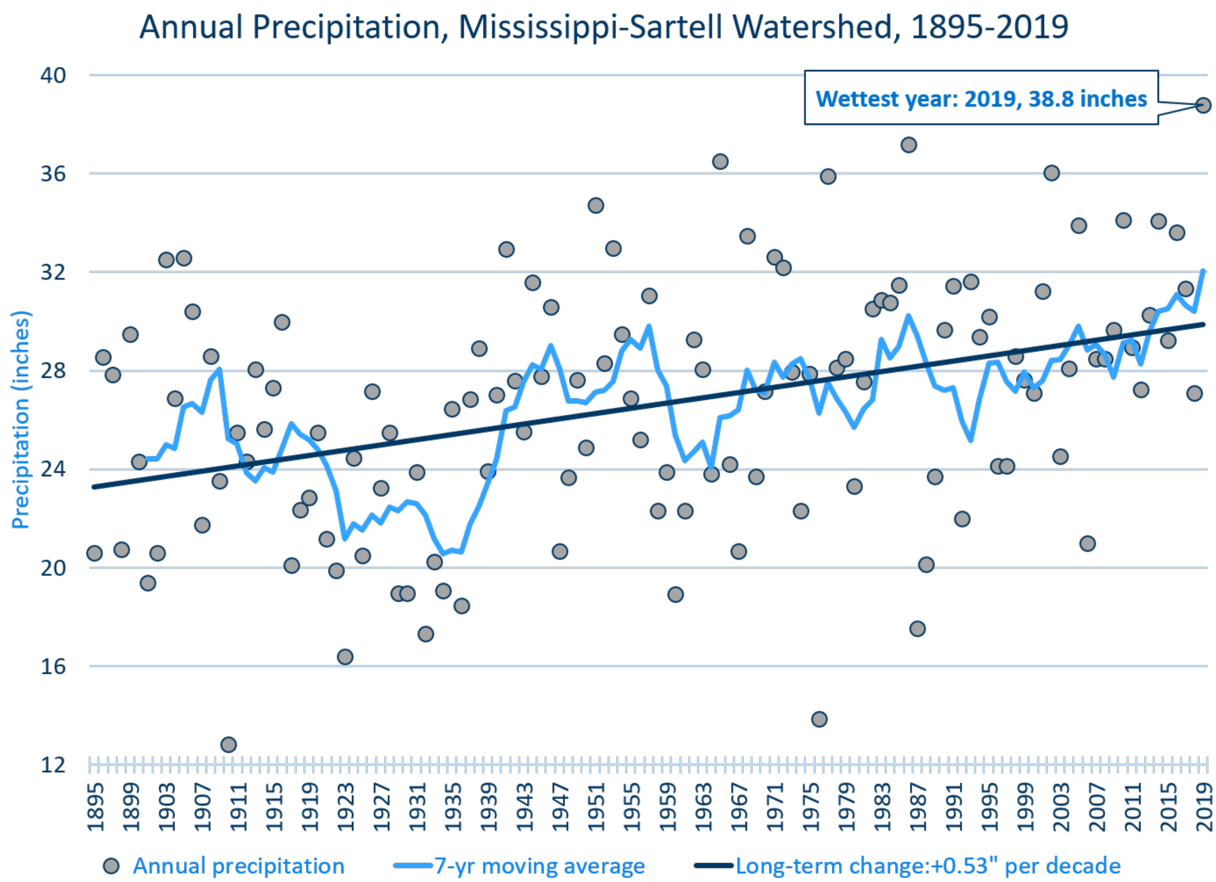

Figure 7

The graph above shows combined annual temperature and precipitation departures for the Mississippi-Sartell Watershed, with the 15 combined warmest & wettest years called out, along with the wettest year on record (2019). Note that 14 of the 15 combined warmest/wettest years have been since 1970. Twelve of 15 have been since 1990. Data from DNR Climate Trends Tool (https://arcgis.dnr.state.mn.us/ewr/climatetrends/#).

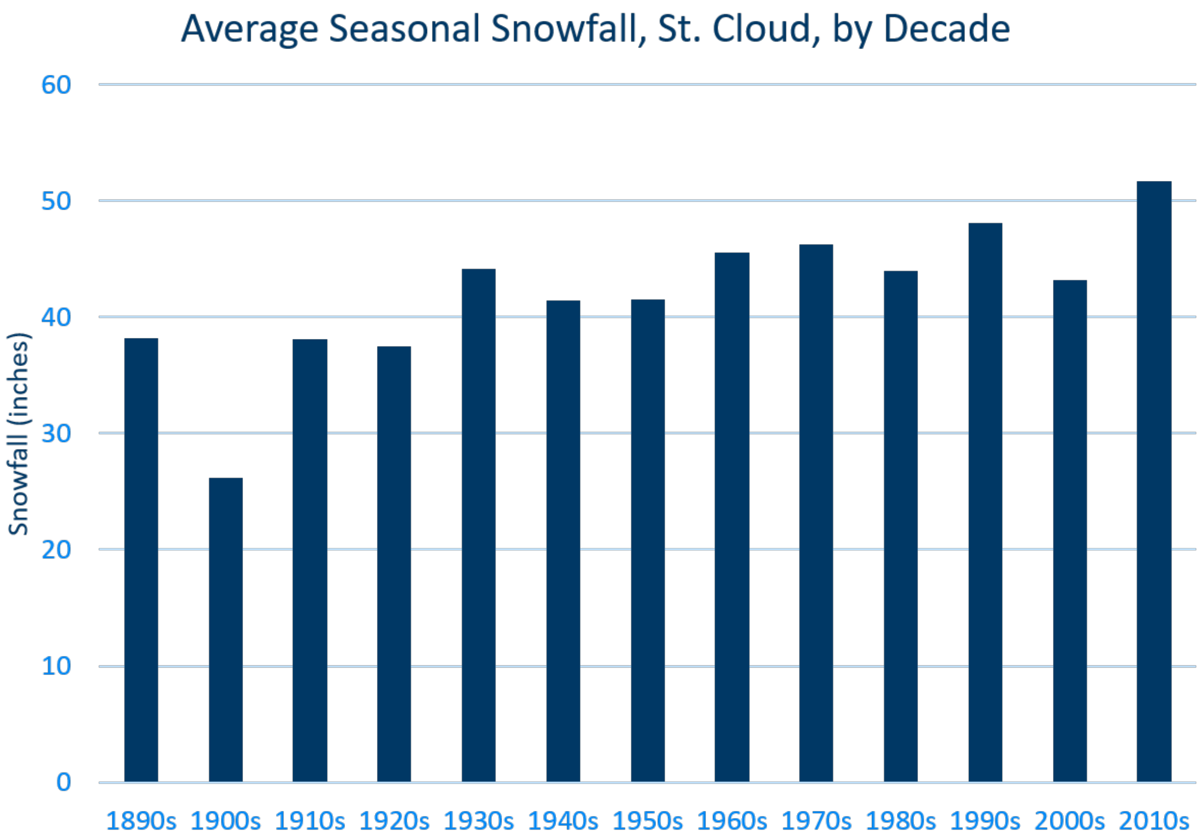

Figure 8

The chart above shows seasonal snowfall by decade for St. Cloud, which is the nearest high-quality long-term station with snow records.

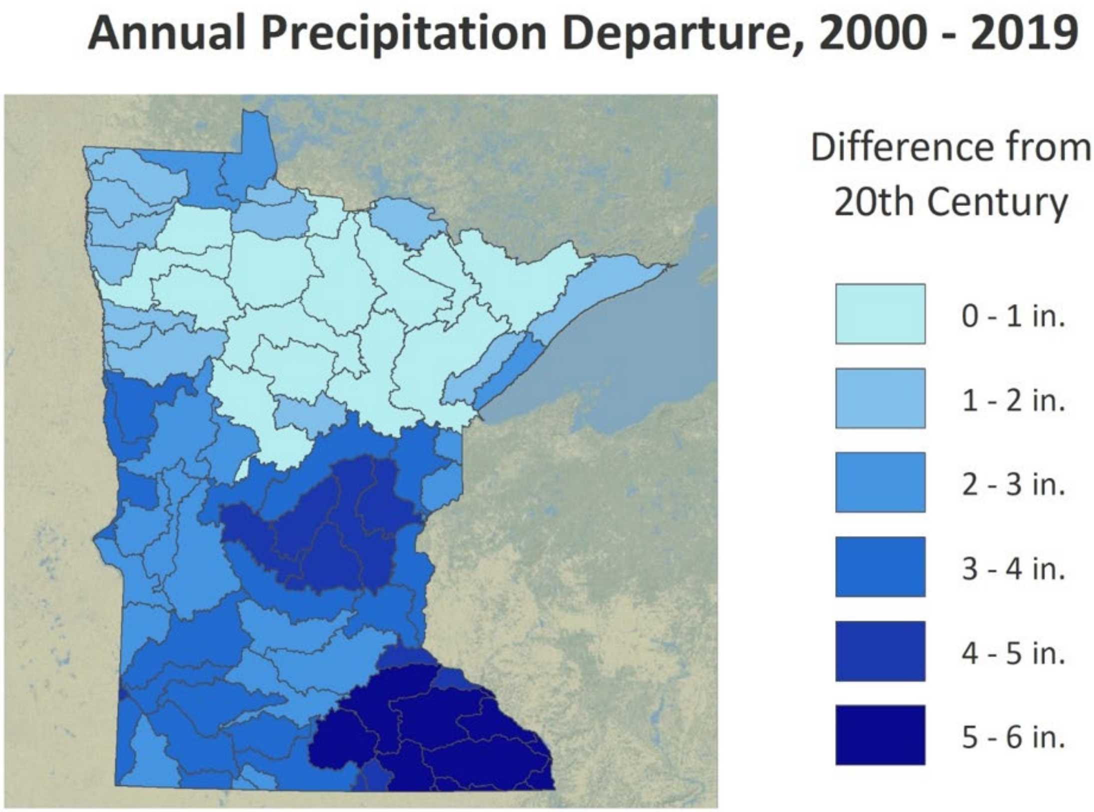

Figure 9

The map above shows precipitation changes by watershed in the period 2000-2019 compared to 1900-1999 averages. Modified from map by DNR Watershed Health Assessment Framework Team.

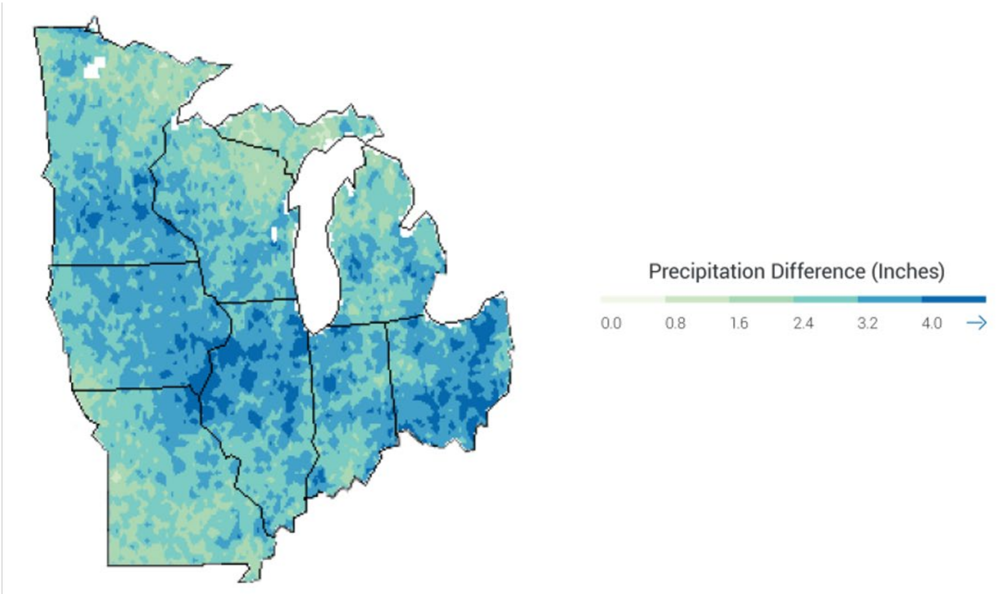

Projected changes in the average annual precipitation
for the middle of the current century (2041-2070) relative to the end of the last century (1971-2000) under continued emissions (A2 scenario).

Source: 2014 National Climate Assessment, Midwest Chapter

Figure 10

Precipitation is projected to keep increasing. Climate models project that these precipitation trends will also continue in the future. The map above shows projected changes in the total annual average precipitation from the 2014 National Climate Assessment. Minnesota shows projected precipitation increases ranging from more than 4 inches in the central region of the state to less than one inch in the northeastern region of the state. Again, we should expect dry years, and even drought along the way, if only because of normal variations in our climate.

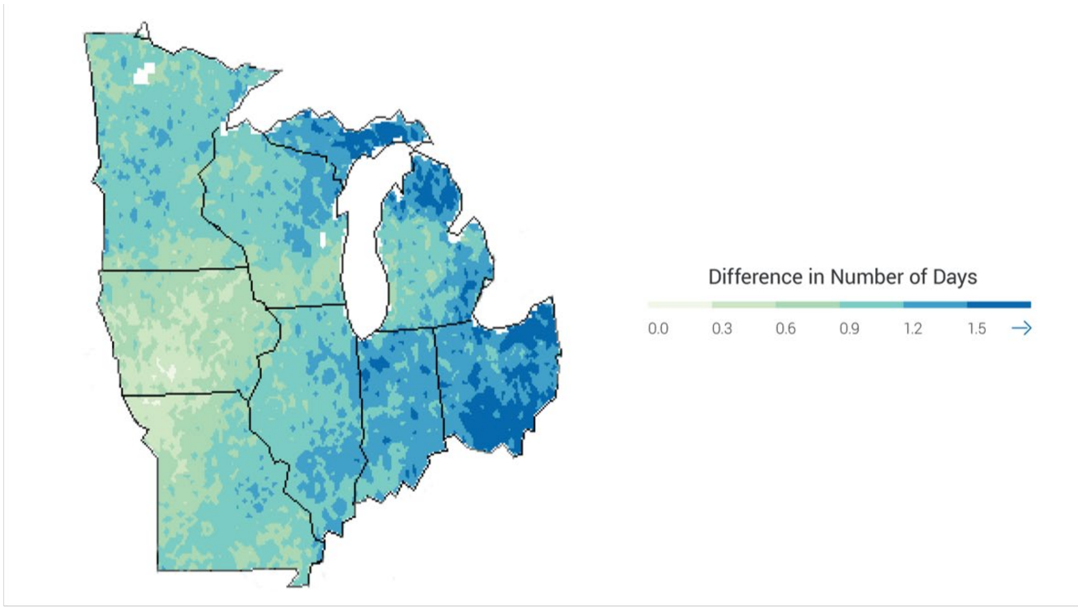

Projected changes in the number of days with very heavy precipitation
(top 2% of all rainfalls each year) for the middle of the current century (2041-2070) relative to the end of the last century (1971-2000) under continued emissions (A2 scenario).

Source: 2014 National Climate Assessment, [Midwest Chapter]

Figure 11

More extreme precipitation is projected. The map above shows how many additional days we expect rainfall within the 98 percentile, or about 2 inches falling in 24 hours, by the middle of this century. On average, we expect to see about one additional day of what is now 98th percentile rainfall. Most parts of Minnesota currently experience one to two days of that type of rain each year, so this kind of increase would mean two to three days total., Our climate always varies from year to year, so we'd expect that some years may not get any of these two inch rains at all, but other years would have many of them, increasing the risk for flooding and other related hazards.

Appendix C – Supplemental Tables

Table C-1 Previously published studies

Reference	Source Organization	Description
Helgesen (1973)	U.S. Geological Survey (USGS)	Field studies and electric analogue model of surficial aquifer in Morrison County
Lindholm (1980)	USGS	Appraisal of the surficial aquifer system in Benton, Sherburne, Stearns, and Wright counties
Ruhl and Cowdery (2004)	USGS	Steady-state models of the surficial (water-table) aquifer along the Mississippi River from Brainerd to St. Cloud developed to support wellhead protection
Hagland (2005)	Minnesota Department of Health (MDH)	City of Rice Part 1 wellhead protection area delineation and vulnerability assessments
City of Rice (2007)	City of Rice	Wellhead protection plan
Delin (2007) and Delin et al. (2007)	USGS	State-wide, average groundwater recharge estimates
Benton SWCD (2009)	Benton County Soil and Water Conservation District	Little Rock Creek stressor identification report
Setterholm (2010)	Minnesota Geological Survey (MGS)	Part A geologic atlas of Benton County (geology)
Rivord (2014)	DNR	Part B geologic atlas of Benton County (hydrogeology)
Lusardi (2014)	MGS	Part A geologic atlas of Morrison County (geology)
Westenbroek (2015)	USGS	State-wide, annual groundwater recharge estimates from a Soil Water Balance (SWB) model
Barr Engineering (2015)	Prepared for Benton SWCD and Minnesota Pollution Control Agency (MPCA)	Total maximum daily load (TMDL) report for Little Rock Creek including surface-water, groundwater-flow, and in-stream water-quality modeling

Table C-2 Stream gaging stations in the Little Rock Creek watershed

Stream	DNR Station No.	Streamflow Data Types	Date Ranges
Little Rock Cr	15029005	Field measurements	2008, 2010-present
Little Rock Cr	15029004	Field measurements	2008, 2010-present
Little Rock Cr	15029003[1]	Field measurements; daily discharge; temperature	Miscellaneous 1968-11 to 1978-09, 2008, 2010-2014 Daily 2014-07 to present
Little Rock Cr	15029001	Field measurements, daily discharge; temperature	Daily, partial years 1998, 1999, 2001, 2003, 2006; Daily, short periods 2000, 2002, 2004, 2005; Daily 2008 - present
Bunker Hill Cr	15028001	Field measurements, daily discharge	Daily 2006-05-03 to 2009-11-05 (missing winter) Miscellaneous 2010-2011
Bunker Hill Cr	15028002	Field measurements	2010 - present
Little Rock Cr	15029002	Field measurements; daily discharge; temperature	Miscellaneous 2008, 2010-2014; Daily 2014-07 to present
Little Rock Cr	15031001[2]	Field measurements; daily discharge; temperature	Miscellaneous 1969-1988, 2007-08; 2010-2014 Daily 2006-06-01 to 2011-09-25 (missing winter); 2017-6-21 to present
Sucker Cr	15026002	Field measurements; daily discharge	Daily 2006-05-03 to 2008-12-16

[1] USGS Station 05268500

[2] USGS Station 05268700

Table C-3 DNR observation wells

Obwell Number	Unique Number	Status	Aquifer Type	Screened Unit(s)	Period of Record	Year Data Logger Installed
49000	243996	sealed	Buried water table	cs2	1969-10 to 2015-06	--
49001	243997	sealed	Water table	Unknown	1973-10 to 1989	--
49002	243998	active	Water table	ou	1968-10 to present	--
49028	431178	active	Water table	ou	1989-10 to present	2012
49003	243999	sealed	Water table	ou	1969-10-6 to 2007-04	--
49004	244000	sealed	Buried artesian	vs	1969-10 to 2012-07	--
49005	244201	sealed	Water table	pgs/ou	1969-10 to 2012-07	--
49008	244204	active	Water table	pgs/ou	1968-10 to present	--
49031	783238	active	Water table	ou	2011-10 to present	2012
49032	789965	active	Buried artesian	es	2012-04 to present	2012
49033	789964	active	Buried artesian (nested with 49034)	es	2012-04 to present	2012
49034	783245	active	Water table (nested with 49033)	ou	2012-07 to present	2012
49035	792505	active	Buried water table	cs2	2014-06 to present	2014

Obwell Number	Unique Number	Status	Aquifer Type	Screened Unit(s)	Period of Record	Year Data Logger Installed
49038	819502	active	Buried artesian (nested with 49039 and 49040)	suu	2016-06 to present	2016
49039	819503	active	Buried artesian (nested with 49038 and 49040)	vs/suu	2016-06 to present	2016
49040	816911	active	Water table	ou/cs2	2016-07 to present	2016
05004	243629	sealed	Water table	ou	1976-10 to 2015-07	2012
05000	243625	sealed	Water table	ou	1976-10 to 2015-07	2012
05005	124157	active	Buried artesian	vs	1978-03 to present	--
05002	243627	sealed	Water table	ou	1976-10 to 2015-07	--
05003	243628	inactive	Water table	ou	1976-10 to 1979-06	--
05006	462820	active	Water table (nested with 05007)	pgs/ou	1990-06 to present	2012
05007	243443	active	Buried artesian (nested with 05006)	es	1990-06 to present	2012
05008	789911	active	Water table/buried	mls	2012-11 to present	2012
05009	792511	active	Water table	ou	2014-08 to present (replaced 05002)	2014

Obwell Number	Unique Number	Status	Aquifer Type	Screened Unit(s)	Period of Record	Year Data Logger Installed
05010	792512	active	Water table	ou	2014-08 to present (replaced 05004)	2014
05011	792513	active	Water table	ou	2014-09 to present (replaced 05000)	2014
05013	819501	active	Buried artesian (nested with 05014)	suu	2016-06 to present	2016
05014	816910	active	Water table	ou/cs3	2016-07 to present	2016

Table C-4 Pumping tests in the Little Rock Creek area in order of test date

Pumping Well(s) Unique No. or Location	DNR Permit No.	Aquifer Type / Pumped Unit(s)	Date	Pumping Length (hrs) / Rate (gpm)	Observa-tion Wells	Properties / Parameters Estimated	Information Source
213460	1969-0518	buried / mlt-es	1970	48 / 1100	unknown	transmissivity, specific yield?	Helgesen (1973)
T39, R32, S1 bbd	--	water table / unknown	1968-70	4 / 45	single well test	transmissivity	Helgesen (1973)
T39, R32, S35 dbc	--	water table / unknown	1968-70	2 / 600	single well test	transmissivity	Helgesen (1973)
124163	1975-3305	water table / ou-mls	Jun 1978	37 / 745	4 unknown	transmissivity, vertical anisotropy, specific yield	Lindholm (1980)

Pumping Well(s) Unique No. or Location	DNR Permit No.	Aquifer Type / Pumped Unit(s)	Date	Pumping Length (hrs) / Rate (gpm)	Observa-tion Wells	Properties / Parameters Estimated	Information Source
150538	1990-3150	buried / es	May 1989	8 / 885	single well test	transmissivity	DNR permit files
139235	1979-3086	water table / ou-cs2-3	June 1989	72 / 600	temp. obwell, Obwell 05002, 504672	transmissivity, specific yield	DNR permit files
227317	1980-3112	buried / suu	June 1989	24 / 800	Pumping well and 2 DO/PC wells	transmissivity, storativity	DNR permit files
473132	1991-3157	buried / suu	May 1991	24 / 360	244710, Rice 1 and Rice 2, "cemetary well"	transmissivity, storativity	DNR permit files
510894	1990-3415	buried / es	May 1991	72 / 990	431170, 431171, 462820, 243443, domestic wells	transmissivity, storativity	DNR permit files
497761	--	buried / es	Oct 1991	9 / 140	single well test	transmissivity	City of Rice
473143	1991-3255	buried / es	June 1993	22 / <250	123327	none	DNR permit files
590742	1998-3119	buried / es	Nov 1998	28 / 290	600839, 600824; 149021, 258156, 526514	transmissivity, storativity	DNR permit files

Pumping Well(s) Unique No. or Location	DNR Permit No.	Aquifer Type / Pumped Unit(s)	Date	Pumping Length (hrs) / Rate (gpm)	Observa-tion Wells	Properties / Parameters Estimated	Information Source
632076	1975-1129	buried / vs-suu	Nov 1999	30 / 600	632075	transmissivity, storativity, leakage factor	MDH
590742, 600824, 600833, 600839	1998-3119	buried / mls-es	Jun 2000	68 / 700 (total)	258156, 526514 (City of Rice wells)	none	DNR permit files
803655	2014-1180	buried / mls?, ebs?	Jan 2014	30 / 250	single well test	transmissivity	DNR permit files
542504	2014-0482	buried / mls	Apr 2015	413 / 123	811553. 811554, 565949, 668632, 484502	transmissivity, storativity, leakage factor	DNR permit files
797177	2013-1345	buried / es-vs	Apr 2015	785 / 168	811557, 811558, 811559, 811560, 668544, 424771	transmissivity, storativity, leakage factor	DNR permit files
749276	2014-2053	buried / vs-suu	Apr-May 2015	615 / 168	811555, 811556, 152072	transmissivity, storativity, leakage factor	DNR permit files
753134	2014-1796	buried / vs	Dec 2015	625 / 95	814736, 814737, 814762	transmissivity, storativity, leakage factor, Beta (aquitard storage factor)	DNR permit files
762210	2014-2014	buried / vs	Jan 2016	562 / 72	814762, 814763, 814736	transmissivity, storativity, leakage factor, Beta (aquitard storage factor)	DNR permit files

Pumping Well(s) Unique No. or Location	DNR Permit No.	Aquifer Type / Pumped Unit(s)	Date	Pumping Length (hrs) / Rate (gpm)	Observa-tion Wells	Properties / Parameters Estimated	Information Source
578703	2015-1184	buried / mls (cs3)	Jan 2016	645 / 71	816439, 816440	transmissivity, storativity	DNR permit files
570935	2014-1952	buried / mls	Feb 2016	375 / 95.5	816441, 816442, 816443, 789964	transmissivity, storativity, leakage factor, Beta (aquitard storage factor)	DNR permit files
579021	2015-1183	buried / es	Feb 2016	392 / 96	816443, 816444, 816441, 789964	transmissivity, storativity, leakage factor, Beta (aquitard storage factor	DNR permit files
683920	2014-1966	water table / ou	Mar 2016	193 / 96.5	816445	transmissivity, storativity, specific yield	DNR permit files

Appendix D – Geological Mapping Methods and Analysis

Bedrock Topography

Existing information and interpretations were considered during re-analysis of bedrock topography. A bedrock valley originating in southern Crow Wing County underlies the central part of the study area and extends into a network of paleo valleys in the Minnesota River valley (Jirsa and Chandler, 2010; Boerboom, 2014). The shape and position of the bedrock valley is partially controlled by the bedrock erodibility. Steeper bedrock slopes and bedrock knolls characterize the eastern side of the valley, where harder igneous rocks intruded into softer schist in western Morrison and northwestern Benton counties (Jirsa and Chandler; 2010, Boerboom, 2014).

Bedrock topography is known with more detail and confidence at higher bedrock elevations where more well borings reached the bedrock surface. There are fewer boring records that reach bedrock within the bedrock valley in much of Morrison County and in the deepest parts of the valley near and southeast of Little Rock Lake. Areas with more data include the area to the west of the valley from Rice to Sauk Rapids, an area of shallow bedrock along Bunker Hill Creek, and an area of shallow bedrock west of Buckman.

The bedrock valley is likely a paleo-drainage feature predating Quaternary glaciation. This conceptual model is supported, for example, by till encountered immediately above the bedrock surface in Morrison County rotosonic boring Mo-06 (Lusardi, 2014) located in the broad bedrock valley southeast of Skunk Lake. Thick sand and gravel deposits encountered in rotosonic and well borings indicate that glacial meltwater streams reoccupied the bedrock valley and its tributaries during the Quaternary.

Deep borings in both Morrison and Benton counties that were constructed or located after completion of the atlas bedrock surfaces were added to previously available data on bedrock elevation. Records for borings that were completed above the bedrock surface but were deeper than the previously mapped bedrock surface were used to estimate bedrock-surface points. Segments of the existing bedrock contours from the atlases were deleted near new data points or where contours were not congruent at the county border. Where new point data were not available, segments of the existing bedrock contours were maintained as inputs to the interpolation. A new bedrock surface grid was interpolated from the resulting point and contour data using the ArcGIS TopoToRaster tool.

Sub-surface Quaternary Geology

MGS geologists interpreted the sequence of glacial advances and associated sub-surface deposits by analyzing rotosonic sediment cores (Setterholm, 2010; Lusardi, 2014). Late Wisconsinan deposits in the area are associated with the northeastern sourced, Superior ice lobe that advanced and retreated from the area two or three times. Most of the Pre-Wisconsinan deposits are of north-northwestern, Winnipeg Provenance, although patches of sediments of northeastern Rainy Provenance may be present in the study area.

The rotosonic samples provided the basis for the stratigraphic framework, but sub-surface mapping was based primarily on information from well records, mostly drilled using the mud-rotary method. The two basic categories of sediments that are the most distinguishable in well-drillers logs are any materials containing clay (e.g. clay, diamicton, silty-clay) and coarse-grained materials containing minimal clay (e.g. sand, gravel, very sandy diamicton) that cause “chatter” during mud-rotary drilling. Sub-surface interpretation of Quaternary geology relies heavily on correlating sand deposits, which are assumed to occur most often on top of clay-bearing tills of the same ice lobe. There were several differences in the organizational framework and lateral correlations of subsurface units between the Benton and Morrison atlases.

Setterholm (2010) grouped some Pre-Wisconsinan units that could not be distinguished from the available data into lumped mapping units in their model of Benton County Quaternary Stratigraphy. In the LRCA, the most significant lumped mapping unit is Qbs/Qsb. They interpreted Qbs to possibly include till (and associated lake sediment) of the Browerville, Lake Henry, and St. Francis formations and Qsb to include pro-glacial sand and gravel deposited primarily during the Emerald phase of the Superior Lobe but also older sediments. Lusardi (2014) did not group stratigraphic units into lumped mapping units for Morrison County, and the Browerville and St. Francis formations were not mapped as present within the Morrison County portion of the LRCA. Of the possible Obs units, only the Meyer Lake member of the Lake Henry Formation was mapped within the study area.

The differences between the Quaternary geological models for the two atlases also differed in the interpretation of the stratigraphic position of some deposits based on differences between the two models in the area where cross sections developed for the two atlases overlap (i.e. the Benton County model was developed using one cross section in Morrison County).

Setterholm (2010) interpreted the base of the Superior Provenance deposits (Cromwell Formation) to have more vertical relief and to extend to greater depths than did Lusardi (2014), particularly over the bedrock valley, whereas deeper parts of these deposits were assigned to older units in the Morrison atlas. The Qsb sand unit in Benton County is laterally coincident with several sand bodies (mls, es, and vs) mapped in Morrison County, with the correspondence varying with location. The es and vs units are expected to be stratigraphically older than Qsb, however.

Geological Mapping Methods and Analysis

The differences in stratigraphic interpretations between the Benton and Morrison geologic atlases were addressed by re-interpreting the subsurface unit surfaces in Benton County within the study area. DNR staff redrew correlation lines on Benton County cross sections within the LRCA using stratigraphic nomenclature and interpretations following the Morrison County atlas. Well logs post-dating the Benton atlas work were added to the cross sections prior to interpretation using the DNR Groundwater Tools add-in for ArcGIS. Therefore, the mapping work was an update to the previous work in addition to re-interpretation.

In addition to well records, surficial geology and geomorphology provide information about shallow sub-surface geology. For example, a north-south trending topographic trough, occupied by Little Rock Creek and Little Rock Lake, was interpreted to signify a sub-glacial tunnel valley that was eroded into older deposits and later reoccupied by surficial glacial meltwater rivers (Setterholm, 2010; Lusardi, 2014). This and other surficial features were retained and considered during interpretations of cross sections.

The vertices of the correlation lines on the cross sections were converted to horizontal points with elevation attributes, also using the DNR Groundwater Tools. Base elevation points for each unit were interpolated into continuous surfaces. Additional points delineating the bottom surfaces of units were added in map view, and some points were modified or deleted to refine the surface interpretations from a three-dimensional point of view.

Benton County cross section 1 is nearly coincident with Morrison County cross section 60. To merge the Morrison model with the newly created surfaces, unit bottom elevations from the Morrison model were interpolated between 500 m north of cross section 1 and data from the new surfaces along cross section 1.

The Morrison County cross sections were not re-interpreted, but several changes were made to the Quaternary unit surfaces in Morrison County to rectify to the modified bedrock topography, remove anomalies, and to ensure that high capacity wells screens were in sand/gravel.

Changes to the bedrock topography affected the way the Quaternary surfaces intersected bedrock in Morrison County. In most places, the bedrock changes could simply be treated as modifying the elevation of the base of the deepest Quaternary unit. At some locations, the new bedrock surface cross cuts one or more Quaternary units. Unit bases were set to equal the bedrock elevation where they overlapped.

The Morrison County till-base surfaces included elevation anomalies at some locations between cross sections. The source of the anomalies appears to be related to the way fully eroded till units and associated sand-body surfaces were generated for the atlas. A mask excluded areas where a map unit is absent from the surface-generation procedure. However, where the mask for an overlying unit, typically the sand unit associated with a till, did not completely cover the "hole" in the till mask, the surface-generation procedure produced anomalous ridges of higher elevation of the till base surfaces. These anomalies were found in all the till unit base surfaces.

At DNR staff request, the MGS provided continuous surfaces of the till bases, derived from the original model data (Robert Tipping, pers. comm.). Where a unit is absent in the model, the base of the continuous surface matches the top of the appropriate underlying unit. These surfaces retained the anomalous ridges of higher elevation. DNR staff applied a three-step process to remove the anomalies. First the surfaces were contoured to five-foot intervals using the ArcGIS Contour tool. Then whole or parts of anomalously high contours were deleted manually in ArcMap. Corrected grids were then interpolated from the modified contours using the ArcGIS TopoToRaster tool.

DNR staff modified the thickness and extent of sand units within Morrison County where new or relocated well data indicated sand was present but sand was not mapped in the published geological surfaces. Most of these new or relocated wells have water-appropriation permits. Therefore, it was important to extend coarse grained materials to the locations of these well screens. These sand-surface changes were accomplished by modifying contours and re-interpolating surfaces from the modified contours, similar to the anomaly corrections. Where sand thicknesses were increased, raster processing was used to ensure that the total sand body thickness did not exceed the total thickness of its formation. Sand thickness grids are shown in Figure 8.

MGS geologists reviewed the modified till-unit surfaces and sand-thickness grids for consistency with the geological framework. They concluded that the till surfaces appear to be consistent with the Morrison atlas surfaces; the sand thicknesses appear to be consistent with the atlas sand maps; and the stratigraphy applied to Benton County is consistent with currently available well records (Robert Tipping, pers. comm.).

Appendix E – Modeling Procedures

Model Construction Procedures

Multiplier and Zone Arrays for Calculating Effective Hydraulic Conductivities

Each model grid cell was assigned to one of three types: 1) only aquifer, 2) both aquifer and aquitard, and 3) only aquitard. For the first and third types, the horizontal and vertical conductivities of the aquifer or aquitard were assigned to the cell and to the quasi-3D “cell”. For the second type, effective values for the horizontal hydraulic conductivity and the vertical hydraulic conductivity were calculated using additive parameters. Multiplier and zone arrays were used to calculate layer transmissivities and vertical conductances in MODFLOW. These arrays were derived from the 30-m stratigraphic model grids using the series of steps as follows.

The model layer elevations were assigned so that only one aquifer and one aquitard hydrostratigraphic unit were assigned to a cell. An exception was in the northeastern part of the model domain where the ct2 and cs2 units were placed in layer 2 instead of layer 1 (See 5.3.2 Vertical Discretization). These geological units are similar to the ct3 and cs3 units, respectively, also in layer 2. Where the ou outwash sand unit extends below layer 1 and is in direct contact with the cs3 sand, the vertical boundary between these units is not distinguishable, and they are lumped in the same hydrostratigraphic unit.

Geoprocessing scripts were developed to calculate 30-m raster grids of the thickness and thickness fraction (unit thickness/total thickness) of each hydrostratigraphic unit within each layer. The saturated thickness of each unit within a raster cell was calculated as the minimum of the unit top, the layer top, or the water-table surface (described above under Discretization) elevation minus the layer bottom elevation.

Then the aquifer fraction (total sand unit thickness divided by total saturated layer thickness) and total aquitard thickness in each 30-m cell in each layer were calculated. The aquifer fraction was mapped from the 30-m raster to the MODFLOW grid by taking the arithmetic average of the 30-m raster values within each MODFLOW cell. The aquitard fraction in each cell was calculated within MODFLOW as 1 minus aquifer fraction. The aquitard fraction in the bottom half of layer 1 was similarly mapped from the 30-m raster to MODFLOW cells.

MODFLOW calculates vertical conductance between cells using the thickness of the bottom half of the upper cell, the thickness of the quasi-3D layer (if present), the thickness of top half of the lower cell, and the vertical hydraulic conductivities of each respectively (See Harbaugh, 2005, p. 5-8). The net effect of all three components is lumped in the value of the vertical conductance.

The quasi-3D layer hydraulic conductivity multiplier was simply 0.1/aquitard thickness as given above because the thickness of the quasi-3D layer was arbitrarily set as 0.1 meter. Where MODFLOW cells contained some 30-m raster cells with zero aquitard thickness, the aquitard thickness in those 30-m raster cells was set to 0.0001 m when calculating MODFLOW cell averages. This results in a multiplier of 1,000 for that 30-m cell, which is a reasonable ratio for aquifer to aquitard vertical hydraulic conductivity.

Irrigation Input

The reported monthly irrigation volumes had to be partitioned into individual irrigation applications for input to the GSSHA model. Crop-irrigation applications may vary from less than ½ inch to more than one inch. Growers may adjust application rates as crop-water-use rates progress through the season. The default application amount was ¾ inch. This default application rate was adjusted when necessary to maintain the correct total monthly volume and realistic timing and number of irrigation applications in each month.

For each permit-month, the number of irrigation events was calculated from the monthly volume and the application rate, with the final application rate adjusted to match the reported volume over the determined number of events. Up to eight potential irrigation events for each month were assigned and ranked in priority based on the timing of rainfall events and position in the growing season. Times after extended periods with no rainfall were given first priority, and so on. It was also assumed that irrigation events in May and September were more likely later/earlier in the month, respectively. This approach did not attempt to rigorously account for crop water needs, but the focus was on applying the reported monthly water volumes via irrigation events at realistic times (i.e. not immediately after significant rainfall events).

In a small number of cases, the reported irrigation volumes appeared to have errors. For a few cases, this appeared to result from water use mistakenly reported in units of millions of gallons rather than gallons (i.e. the reported volume multiplied by one million was appropriate for the permit). Several reported crop irrigation volumes were unreasonably high (i.e. greater than 20 inches). It was assumed that these were a result of reporting errors. For these cases, the median application rates for all permits for the same year were applied instead of the reported volumes. Additionally, a few of the reported volume data included only the annual total without monthly totals. For these, the annual total was distributed according to the median monthly fractions for all crop irrigation permits. In general, only irrigation uses in May through September were applied in the model. If a very small amount of use was reported for one of the shoulder months, it was combined with the use in the adjacent month since the exact timing of the applications was unknown (i.e. a single application could occur across two different months).

The resulting time series of irrigation applications had to be distributed to individual model cells. The delineated polygons for each irrigation permit were intersected with the base, 200-m model grid to assign groups of model cells to each permit using ArcMap. These were manually checked and cells were added or removed to make the total area of each group of cells representing an irrigated field match the delineated area as closely as possible (each model cells is approximately 9.9 acres).

Finally, a computer program was written to create irrigation time series formatted for input to GSSHA. The inputs were the monthly irrigation volumes for each permit, number of cells for each permit, the irrigation-date priority rankings, and the maximum possible number of cycles for each month. The output was a set of time series indicating irrigation rates and times for each permit. The cells to which each time series applied were designated in GSSHA using an index table.

Recharge Routing

Percolation of water through the unsaturated zone above the water table is a nonlinear process because the unsaturated hydraulic conductivity varies with soil moisture content. Below the root zone, soil moisture is less variable and generally fluctuates between the field capacity and near saturation. Under these conditions, a linear (i.e. independent of initial soil moisture) transfer function, analogous to a unit hydrograph used in surface-water hydrology (NRCS-USDA, 2007), can be an effective approximation for routing recharge. Like a unit hydrograph, the transfer function has an area under the curve (representing recharge amount) of one (1), which is scaled to the actual infiltration amount.

Based on the model of routing through a series of linear reservoirs, a gamma distribution function with initial lag time has been applied successfully (e.g., O'Reilly, 2004). The key characteristics of the gamma distribution are that it has a steeper rising limb followed by a more slowly decaying falling limb.

The LRCA model applied monthly stress periods. Therefore, the detail of sub-monthly timing of recharge was not needed. To rout recharge over monthly stress periods, a simple, triangular transfer function with steeper rising limb and more slowly decaying falling limb was applied, analogous to the triangular unit hydrograph used in surface-water hydrology (NRCS-USDA, 2007). The triangular function is defined by the time to peak (t_p), the peak rate (q_p), and the total time (t_b). There can also be a time lag before any recharge reaches the water table. Like a unit hydrograph, the total area under the triangle is one (1).

Appropriate values for the parameters were selected through evaluation of water-table observation-well hydrographs completed at locations with varying depths to the water table (DTW) in Central Minnesota. The hydrographs were reviewed to find hydrograph segments that were a discrete response to a storm event. The time to the hydrograph peak and approximate length of the recharge event were compared to the depth to the water table. Interestingly, the observation-well hydrographs generally responded within a day or two of precipitation events, even when the water table was more than 25 feet (8 meters) below the land surface. Standard models of unsaturated flow would predict longer lag times before the leading edge of a recharge pulse could reach the water table at these depths. The observed responses may be due, in part, to preferential pathways that quickly saturate, yielding a rapid hydraulic response.

Based on review of hydrographs and the shapes of gamma transfer functions, the shape of the triangle was set such that its area was divided into 25 percent before the peak and 75 percent after. The time to the peak was set to:

$$t_p[\text{days}]=(3\times \text{DTW}[\text{meters}])\text{-}2$$

To maintain the ratio of the areas before and after the peak:

$$t_b=4\times t_p$$

$$q_p= {}^{2}/_{t_b}$$

History-Matching Statistics

The statistical measures listed in Table 9 were calculated as follows:

$$\mathrm{ME}=\frac{1}{n}\sum(o\text{-}s)$$

$$\mathrm{NSE}=1-\frac{\sum(o\text{-}s)^2}{\sum(o\text{-}\bar{o})^2}$$

$$\mathrm{PBIAS}=100\left[\frac{\sum(o\text{-}s)}{\sum(o)}\right]$$

$$\mathrm{RMSE_n}=\frac{1}{(o_{max}\text{-}\ o_{min})}\sqrt{\frac{1}{n}\sum(o\text{-}s)^2}$$

$$\mathrm{RSR}=\frac{\sqrt{\sum(o\text{-}s)^2}}{\sqrt{\sum(o\text{-}\bar{o})^2}}$$

where

ME is the mean error or residual

n is the number of observations

o is an individual observation

s is an individual computed value

NSE is the Nash-Sutcliffe efficiency

$\bar{o}$ is the mean of the observed values

PBIAS is the percent bias

$RMSE_n$ is the scaled root-mean squared error (RMSE)

o_{max} is the maximum observed value

o_{min} is the minimum observed value

RSR is the ratio of the RMSE to the standard deviation of the observations.

Appendix F – Evaluation of Evapotranspiration Estimates

Evaluation of Evapotranspiration Estimates in the LRCA Using Ag Weather Station Data for 2015 and 2016

Introduction

The computed impact of groundwater use on groundwater discharge to Little Rock Creek was sensitive to water balances in irrigated versus non-irrigated fields for different crop types. Differences in soil-water balances were largely controlled by differences in evapotranspiration (ET) with and without irrigation and among different crop types.

ET can be estimated accurately from field measurements using lysimeters or the eddy-correlation (or eddy-covariance) method. These methods require expensive and labor intensive data collection, are limited to a small areal footprint, and are rarely available. ET is usually estimated using models that use more readily available climate data collected at a limited number of stations to calculate potential ET (PET) as the basis for ET estimates.

To further test and evaluate the ET analyses that supported development of the GSSHA model, climate data available for 2015 and 2016 were applied in analysis using alternative ET estimation methods. The ET estimates were also compared to field studies reported in the literature on ET from irrigated corn in Central Minnesota and ET from corn and soybean in Eastern Nebraska.

Data

ET Measurements

There are limited reports in the literature on field-measured ET in central Minnesota or the surrounding region. Dylla et al. (1980) measured water balances in irrigated corn at Westport from 1975 through 1978. Westport is located approximately 50 miles west of the Little Rock Creek Area (LRCA). Soil at the site is Estherville (sandy loam over sand). Percolation below the root zone was measured using 24 non-weighing lysimeters; soil moisture was measured with a calibrated neutron probe; and precipitation was measured with a rain gage. Corn was sprinkler irrigated in 1975 and drip irrigated in 1976 through 1978. ET amounts were plotted from emergence (late May) through estimated maturity date (mid-September). There was significant crop damage due to severe storm and/or fungal disease in 1977 and 1978. There was also some hail and wind damage in August 1975.

Suyker and Verma (2009) report on year-round eddy covariance flux measurements of irrigated continuous corn, irrigated corn-soybean rotation, and rainfed corn-soybean rotation in eastern Nebraska from 2001 through 2005. The eddy covariance method calculates ET from high-frequency measurements of 3-D wind speed and water vapor and is one of the most accurate methods for measuring ET and other trace gas fluxes. Although there are climatic differences between eastern Nebraska and central Minnesota, this study provides high quality data for comparison of seasonal water demand from these annual crops. Soils at the sites are deep silty clay loams. Irrigation water was provided by center-pivot systems. Since initiation in 2001, all of the fields were under no-till (except irrigated continuous corn in 2005). ET totals were reported for planting (early to mid-May for corn and late May to early June for soybean) to harvest (mid- to late-October for corn and early to mid-October for soybean) periods and on an annual basis (planting to planting).

Climate Data

The Little Rock Creek Area (LRCA) model used temperature, humidity, wind speed, and sky cover data collected at the Little Falls/Morrison County or St. Cloud Regional airport (See Appendix A). Measured solar radiation data are not available in the LRCA prior to November 2014. The model used sky cover data to calculate incoming solar radiation. Wind speed at airports is measured from towers 9 or 10 meters (30 to 33 feet) high, but can be adjusted to represent wind speed above the crop canopy.

The Minnesota Department of Agriculture (MDA) partnered with the East Otter Tail Soil and Water Conservation District (EOT SWCD), Pope County SWCD and Benton County SWCD to install 12 weather stations in agricultural settings in central Minnesota to provide data for estimating crop water use (Central Minnesota Ag Weather Network). The stations measure temperature, humidity, wind speed, incoming solar radiation flux, and rainfall on an hourly basis. Two of these stations began operating near Little Falls and Rice (within the LRCA) in November 2014. The DNR obtained archived, hourly records for the Little Falls, Rice, and Westport stations from the MDA (Luke Stuewe, pers. comm.). The solar radiation data collected at the Ag Weather Network stations provide direct measurements not otherwise available.

There is feedback between humidity, temperature, and ET. The location of a meteorological station can affect calculation of PET. Dry air blowing over an irrigated field becomes moister and slightly cooler down-wind from the edge of the field with corresponding reduced evaporative demand down wind. At a sufficient distance from the field edge, the humidity and ET come into equilibrium. Reference PET (See Methods below) is calculated to represent well-watered reference conditions. ET estimation methods based on climate-station data assume that conditions measured at the station represent the conditions at the estimation site. This is generally a reasonable assumption for the Ag Weather Network stations.

Other sources of calculated solar radiation data could also be tested for the period before the Ag Weather Network stations were established. Two types of calculated data are weather-model reanalysis datasets and solar radiation models. Reanalysis datasets consist of weather model forecasts after assimilation of weather-station data and satellite-derived products. Fuka et al. (2013) applied the National Centers for Environmental Prediction (NCEP) Climate Forecast System Reanalysis (CFSR) dataset to watershed models. The CFSR data processed for model input are available from January 1979 through July 2014 and are available from the Texas A&M University spatial sciences website (https://globalweather.tamu.edu/). Another source of solar radiation estimates based on satellite data is the Physical Solar Model (PSM) developed for the National Solar Radiation Database (Sengupta et al., 2014).

To check the potential utility of the CFSR radiation data in Minnesota, CFSR daily radiation totals at the nearest grid point were compared to solar radiation data measured at the University of Minnesota (UMN), St. Paul campus. A regression of the daily CFSR data against the UMN data produced a relatively close fit (slope =0.96; intercept = 0.84; R^2 = 0.82; mean bias error = -8%). When the data are summed over weekly periods, the regression improves (slope = 1.04; intercept = -0.30; and R^2 = 0.93; and mean bias error = -0.02%). The CFSR product that incorporates multiple sources of data appears to provide useful solar radiation estimates. Sengupta et al. (2015) compared data outputs from the PSM to ground-based measurements at 7 stations in the U.S. from 2005 through 2012. The statistics for the CFSR data versus the UMN data fall within the range of station statistics reported for the PSM data validation. Outputs from both models provide additional options for estimating solar radiation during the period before direct measurements became available.

Plant Growth and Development

Plant growth and development through the growing season is an important control on ET. ET increases as crops grow, and ET decreases as plants mature and undergo senescence or go dormant in the fall. These factors have to be represented in some way in any method used to estimate ET.

Crop growth and development depends on crop variety, planting date, and weather during the growing season. Crop planting dates are generally later from south to north across Minnesota and depend on soil moisture conditions, expected time to maturity, and frost risk. The USDA Agricultural Statistics Service Minnesota Field Office publishes weekly crop progress reports from April through October. Representative crop planting dates were estimated for 2015 and 2016 from these reports, assuming that corn and soybean planting in the LRCA typically occurs after 50% of the crop acres in the state have been planted. Crop maturity and harvest dates were estimated similarly, although expected growing season length was also considered as described below.

Temperature effects are tracked by calculation of growing degree day (GDD) units also known as heat units. GDD is calculated as the cumulative sum of the difference between the daily average temperature and a base temperature, with a threshold maximum temperature. Negative values (i.e. daily average temperatures below the base temperature) are set to zero.

Corn growth is strongly controlled by temperature, and growth stages after planting generally track with accumulated GDD (Abendroth et al., 2011). Hicks (2004) provides typical growth versus GDD relationships for Minnesota. Soybeans are sensitive to day length and varieties with different maturity dates are selected by latitude (University of Minnesota Extension, 1999). Akyuz et al. (2017) developed a GDD model for soybean maturity groups that overlap with those recommended for Central Minnesota. The GDD value required for maturity in this model was also considered when defining soybean growing season.

In Minnesota, most growers cut newly seeded alfalfa twice and established alfalfa three times during the growing season (North Central IPM Center, 2000). Some growers also cut alfalfa late in the fall after dormancy. Daily minimum temperatures above -4° C (25° F) (Allen et al., 1998) and/or soil temperature above 4° C (40° F) (Noland et al., 2015) are used as indicators of spring growth in alfalfa. Based on these indicators, established alfalfa typically begins growing four to six weeks before corn emergence and five to six weeks before soybean emergence in Central Minnesota. Therefore, alfalfa typically reaches near full canopy cover before corn and soybeans have emerged, and the first cutting of alfalfa is typically in late May to early June. Alfalfa remains green and continues to transpire until the first killing frost, typically in October, several weeks after annual crops have died and begun drying out.

Modeling Analysis

Two types of ET calculation methods were applied: indirect calculation using crop coefficients and direct calculation using a plant-soil system model. Crop coefficient methods are typically applied for irrigation management, and MDA staff recommended applying this approach for comparison with other methods (Jeppe Kjaersgaard, pers. comm.). Crop coefficient methods are generally limited to the growing season, and, therefore, cannot be used to estimate annual or long-term ET totals.

Solstad (Appendix A) used the WEPP model to estimate ET relationships among different crops under irrigated and non-irrigated conditions during development of the GSSHA model for the LRCA. The WEPP model includes components for calculating plant growth, management schemes, and soil water-balance components among other capabilities.

The Soil and Water Assessment Tool (SWAT) model is a hydrology and water-quality model that has been continuously developed since the early 1990s (Neitsch et al., 2011). It is widely used for watershed-scale hydrologic and water-quality assessments in agricultural watersheds (Arnold et al., 2012). SWAT includes soil, plant, ET, and management components similar to WEPP and comes with an extensive database of plant/crop properties. SWAT was selected to provide another model for comparison with results from the other methods.

Potential Evapotranspiration (PET)

PET represents ET from a surface with unlimited water supply. PET is controlled by plant and soil properties in addition to climate. There are two general approaches to calculating and applying PET: 1) calculating a reference PET for an idealized reference crop that is multiplied by crop coefficients unique to a particular plant and 2) directly calculating PET using parameters that account for plant type and growth. Actual ET (AET) is determined by reducing PET to account for limited water availability and other stresses, although the crop coefficient method is typically applied only when AET is essentially equal to PET.

There are several methods to estimate PET based on combining equations that account for the energy budget at the land surface and mass-transfer of water vapor from the surface to the atmosphere. The Penman-Monteith (PM) form of the combination equation (Monteith, 1965) includes aerodynamic and surface resistances that regulate the rate of transpiration. The PM method has been recommended for use in irrigation management by the FAO (Allen et al., 1998) and the ASCE (ASCE-EWRI, 2005). The PM method is used in GSSHA and is an option in other watershed models including WEPP and SWAT. The

PM method requires temperature, humidity (or dew point), wind speed, and incoming solar radiation data. With the exception of surface resistance, the parameters of the PM equation are determined from meteorological measurements and, typically, using standardized computational procedures (Allen et al., 1998).

The surface resistance (or canopy resistance) describes the bulk resistance to vapor flow through the transpiring leaves and soil surface. Under full cover of vegetation, the canopy resistance is typically related to the stomatal resistance of sunlit leaves and an empirical estimate of the active (sunlit) fraction of the leaf area index (LAI). More complex approaches to representing the leaf canopy are being researched (e.g., Ding et al., 2014). Canopy resistance also varies with meteorological and soil-moisture conditions that affect plant physiology and may vary somewhat throughout the day (Jarvis, 1976; Stewart, 1988; Ball et al., 1987).

Some of the variability in canopy resistance is complex and difficult to measure or must be calculated indirectly, and applying an average or smoothed canopy resistance is typically sufficient to estimate ET at daily and longer time scales without directly accounting for all of the potential variables. When applying the PM method on a sub-daily basis, two canopy resistance values are typically used, one applied during the day and the other at night (e.g. ASCE-EWRI, 2005). The effect of soil moisture deficit on transpiration is typically represented by adjusting AET after PET is calculated rather than directly adjusting canopy resistance. Another adjustment made by the SWAT model is to increase canopy resistance when the vapor-pressure deficit (“dryness” of the air relative to saturation) is above a threshold value, representing the way plants react to very dry air.

For the crop coefficient methods, PET is calculated for a theoretical reference-crop using standardized values of crop height, stomatal resistance, and LAI to calculate aerodynamic resistance and canopy resistance. The reference crop represents a vigorously growing, uniform crop even during time periods when actual crops may not be growing or fully grown. Crop coefficients have been developed for reference-crop parameters representing short grass (short reference crop) and alfalfa (tall reference crop).

Hourly ASCE-EWRI (2005) standardized tall (ET_{rs}) and short (ET_{os}) crop reference ET values were provided with the Ag Weather Network data. Most crop coefficients were developed from daily data and do not vary diurnally. Therefore, daily meteorological variables were extracted from the Rice dataset, and reference ET values were then calculated using daily time steps according to ASCE-EWRI (2005). Daily totals of hourly calculated reference ET are similar to, but typically slightly less than reference ET calculated on a daily time step (ASCE-EWRI, 2005). For the Rice station, May through September ET_{rs} calculated on daily times steps was 1.09 and 1.07 times hourly summed ET_{rs} in 2015 and 2016 respectively.

Crop Coefficient Methods

Crop-coefficients are multiplied by reference PET to calculate ET for a given crop. The simplest approach uses a single, seasonally varying crop coefficient (Kc) for a healthy crop not short of water. These mean crop coefficients are applicable to specific conditions that may vary with climate and soil type, although procedures for adjusting coefficients based on typical humidity and wind-speed conditions have been developed for the FAO-56 method (Allen et al., 1998).

The dual crop-coefficient method uses a basal crop coefficient that primarily accounts for transpiration and a soil evaporation coefficient. The basal crop coefficient varies with crop stage similar to a single crop coefficient, but the soil evaporation coefficient varies with soil moisture and must be calculated using a soil evaporation model. The FAO-56 method describes procedures for applying a soil evaporation model on a daily time step (Allen et al., 1998). This method requires several soil parameters, an estimate of canopy cover for each rain/irrigation event, and a sequence of calculations for every rain/irrigation event.

MDA staff recommended using the ASCE-EWRI (2005) standardized reference evapotranspiration for a tall crop (ET_{rs}), computed from meteorological measurements collected at Minnesota Ag Weather Network stations (Jeppe Kjaersgaard, pers. comm.). Kjaersgaard also cited single crop coefficients developed at Kimberly, Idaho as a potential source for crop coefficients (Allen and Wright, 2002). Based on this and the relative simplicity of the single coefficient method, single coefficients were used for this evaluation.

The Kimberly coefficient set includes values for corn and alfalfa but not for soybeans. Crop coefficients are defined in two sets, before and after effective cover. Alfalfa crop coefficients are defined for first, intermediate, and last cutting cycles. These coefficients will be referred to as K_{crK}.

FAO-56 (Allen et al., 1998) provides grass-based crop coefficients for many crops which can be used with the short reference crop version of the standardized ASCE-EWRI equation (ASCE-EWRI, 2005. p. 47). These coefficient sets include initial, mid-season, and end-season values with linear interpolation between stages. Because soil evaporation is a large fraction of ET during the initial period, the initial value is calculated using a procedure that approximately accounts for soil wetting events throughout the initial period. The resulting initial coefficient can vary widely depending on the average frequency and magnitude of wetting events during the initial period. The resulting coefficient for the initial period also affects the interpolated coefficient between the initial and mid stages (the development period).

FAO-56 based coefficients will be referred to as $K_{co\text{-}FAO}$. Alfalfa-based crop coefficients can be approximately calculated from the grass-based coefficients by dividing by the mid-season grass-based coefficient for alfalfa (1.2). These FAO-56, alfalfa-based coefficients ($K_{cr\text{-}FAO}$) were calculated for comparative purposes, but were not used to calculate ET.

The University of Nebraska Extension provides alfalfa-based crop coefficients by growth stage for several crops including corn, soybeans, and alfalfa. These crop coefficients were applied using estimated growth stage dates and linearly interpolating coefficients between stages. These crop coefficients will be referred to as K_{crN}.

Crop Coefficient Results

ET was calculated using the alternative sets of crop coefficients for corn, soybeans, and alfalfa using the Rice station data for 2015 and 2016. The ET_{rs} based crop coefficients are plotted in Figures F1-F3. Note that for calculating ET using the FAO-56 method, ET_{os} was multiplied by $K_{co\text{-}FAO}$ coefficients, but the corresponding $K_{cr\text{-}FAO}$ values are shown to directly compare with the other ET_{rs} based coefficients.

The crop-coefficient based estimates are less reliable during the initial growth phases and are not calculated prior to planting or after harvest. Because corn and soybeans emerge in late May and have died by the end of September, crop-coefficient-based ET was compared for the months of June through September.

The June through September totals for 2015 and 2016 are shown in Figures 4 and 5. These calculated crop ET values vary from 17.5 to 21.2 inches. From June through September, ET from alfalfa is similar to ET from corn and soybeans, with the different crop coefficient sets resulting in calculated alfalfa ET both higher and lower than calculated ET for the annual crops. Seasonal soybean ET is generally slightly less than corn ET.

The growth patterns of each crop (and alfalfa) affect the calculated ET for June through September, but they also affect ET during the remainder of the season. A longer growing season combined with similar June through September ET results in higher annual ET for alfalfa compared to corn and soybeans. This is not reflected in the June through September totals. The crop coefficient methods cannot be used to calculate and compare total annual ET.

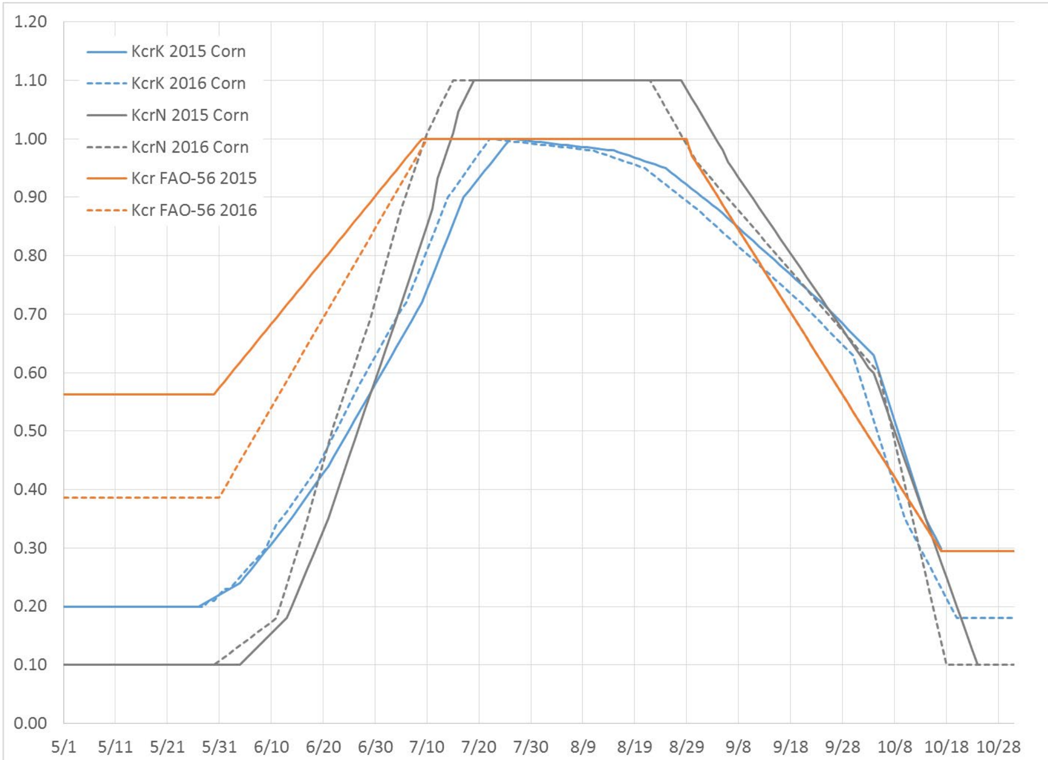

Figure F12 Crop coefficients for corn for 2015 and 2016

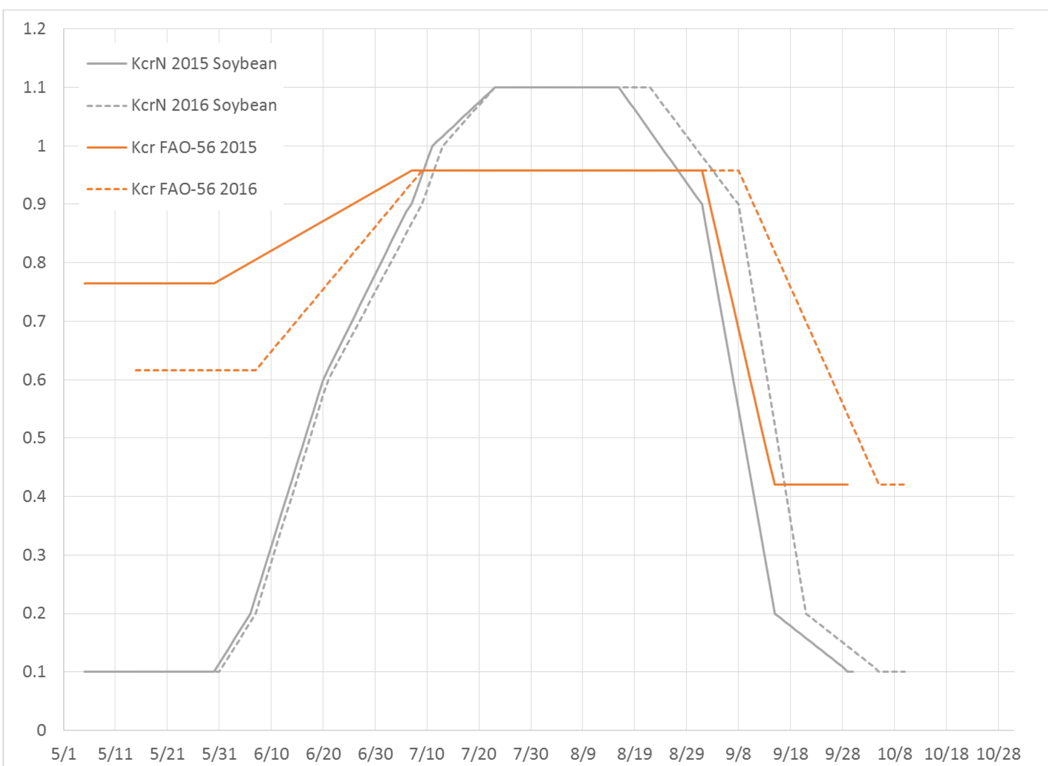

Figure F13 Crop coefficients for soybeans for 2015 and 2016

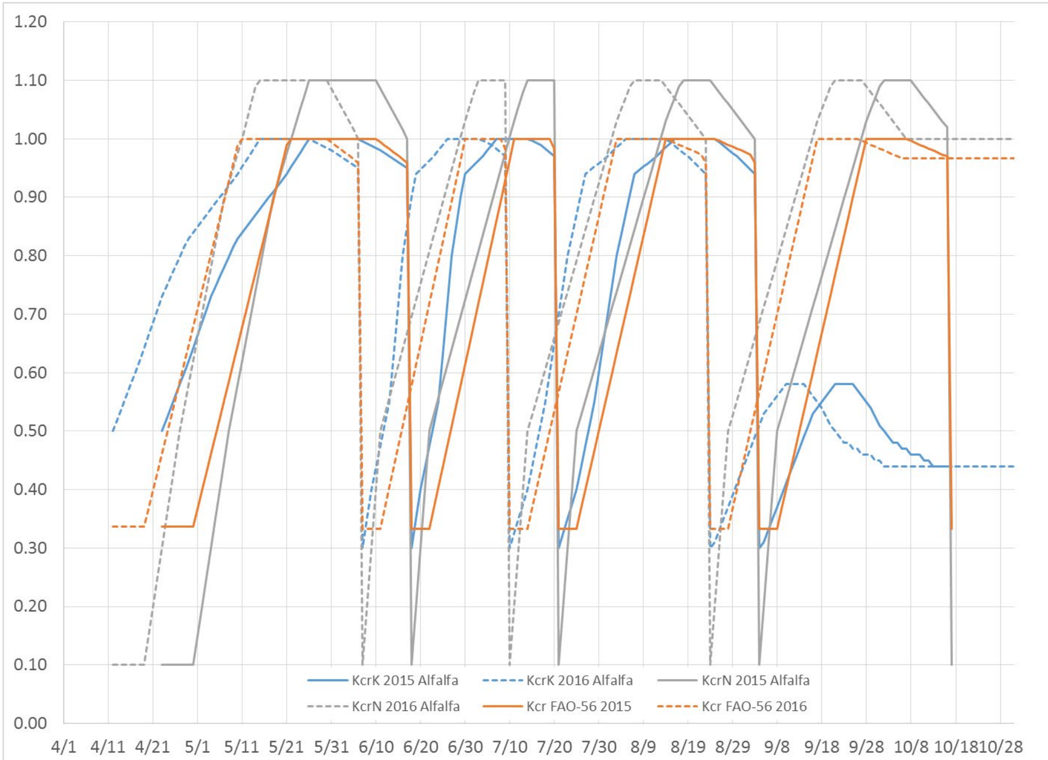

Figure F14 Crop coefficients for alfalfa with three cuttings during the growing season for 2015 and 2016

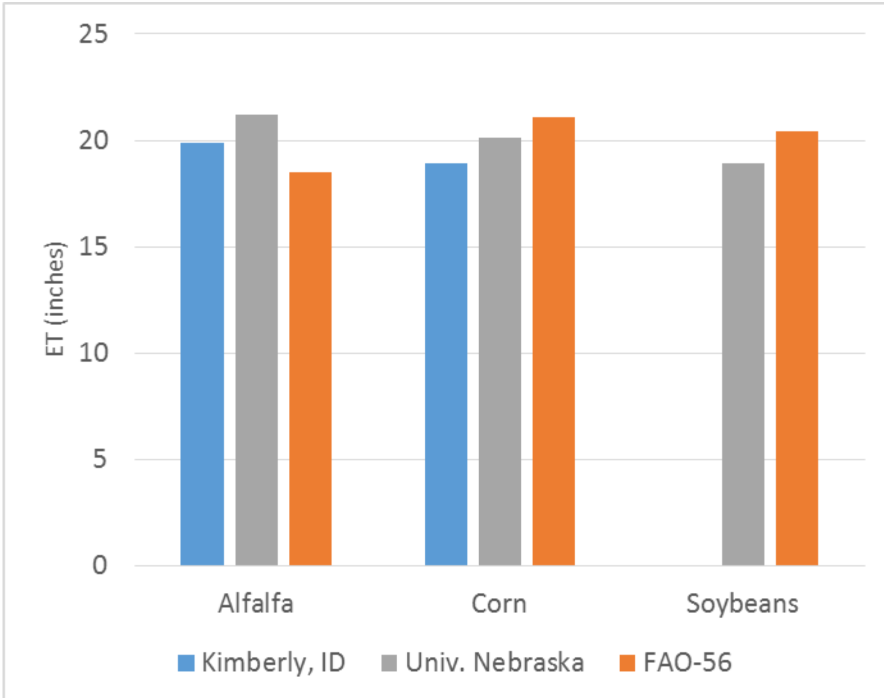

Figure F15 June through September 2015 ET calculated using crop coefficients

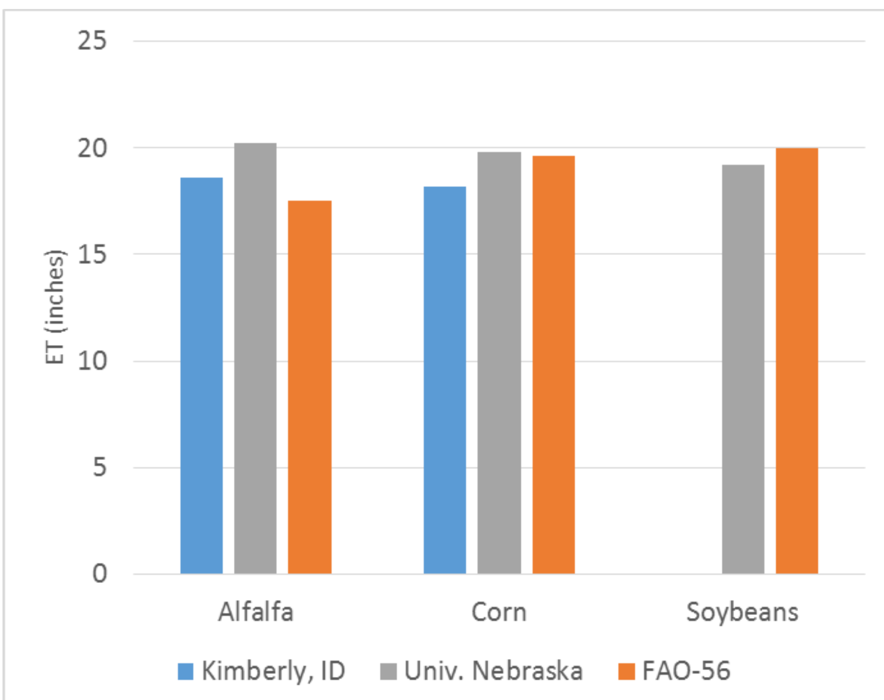

Figure F16 June through September 2016 ET calculated using crop coefficients

SWAT

The SWAT (Soil and Water Assessment Tool) model is a semi-distributed, process-based watershed model that has been developed since the early 1990s, incorporating key components from USDA Agricultural Research Service (ARS) models (Neitsch et al., 2011; Arnold et al., 2012). For most applications, it is run on a daily time step. Two SWAT components that are important to simulation of evapotranspiration are multi-layer soil-water accounting and a plant-growth model. SWAT includes representations of canopy interception, runoff, infiltration, soil and canopy evaporation, and plant transpiration from the root zone among other capabilities.

To compare with the crop coefficient methods, SWAT was run for 2015 and 2016 using the meteorological data from the Rice Ag Weather Station and precipitation from the St. Cloud Regional airport. A burn-in period began in April 2014 using weather station precipitation and temperature data and model-generated values for other weather data prior to the beginning of records at the Rice station in November 2014.

The model was run with and without irrigation for alfalfa, corn, and soybeans and representing two common soils in the LRCA. The Hubbard loamy sand formed in sandy outwash and alluvial sediments, and it consists of 1 to 3 feet of loamy sand over sand. Hubbard soils are assigned to Hydrologic Soil Group A (USDA-NRCS, 1997, 2017). The Pomroy loamy fine sand formed in a mantle of outwash or eolian sediments over dense loamy till, and it consists of 1.5 to 3 feet of loamy fine sand/sand over sandy loam. Pomroy soils are assigned to Hydrologic Soil Group C because of the relatively low permeability of the B- and C-horizons that formed in till.

Model parameters were generally set to the default values. Total GDD to maturity and planting dates for corn and soybeans were set to approximately match the growing season timing applied in the crop-coefficient analyses. Alfalfa was planted in 2014 and cut three times during the growing season in 2015 and 2016. The automatic irrigation option in SWAT was applied so that the total soil water deficit in the active root zone was generally prevented from exceeding 50 percent of the total available water content at field capacity. The results were very similar for the Hubbard and Pomroy soils. The Hubbard soil ET totals for June through September and for the entire year are shown in Figures 6 and 7.

June through September 2015 ET computed by SWAT was 14.1 to 16.0 inches for the irrigated crops, lower than ET computed using crop coefficients. June through September 2016 ET computed by SWAT was 17.6 to 20.2 inches for the irrigated crops, overlapping with the crop-coefficient-based values. Computed June through September ET was slightly higher for corn and similar for alfalfa and soybeans.

The model applied 2 to 4 inches of irrigation water in 2015 and 4.5 to 6.5 inches in 2016. These irrigation totals are comparable to reported irrigation totals for irrigated row crops in the LRCA in 2015 and 2016. Precipitation events were generally timely during the 2015 and 2016 growing seasons, however, preventing extensive soil water deficits even without irrigation. As a result, computed crop stresses and reduced ET without irrigation were minimal.

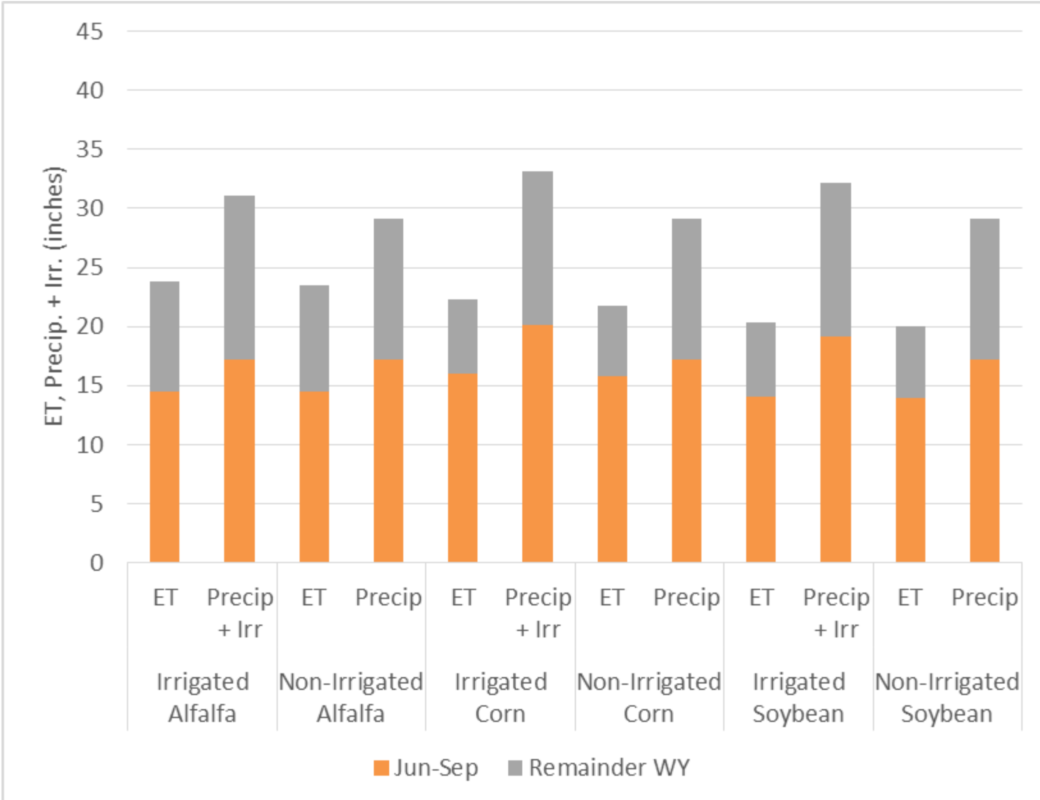

Figure F17 ET computed by the SWAT model for water year 2015.

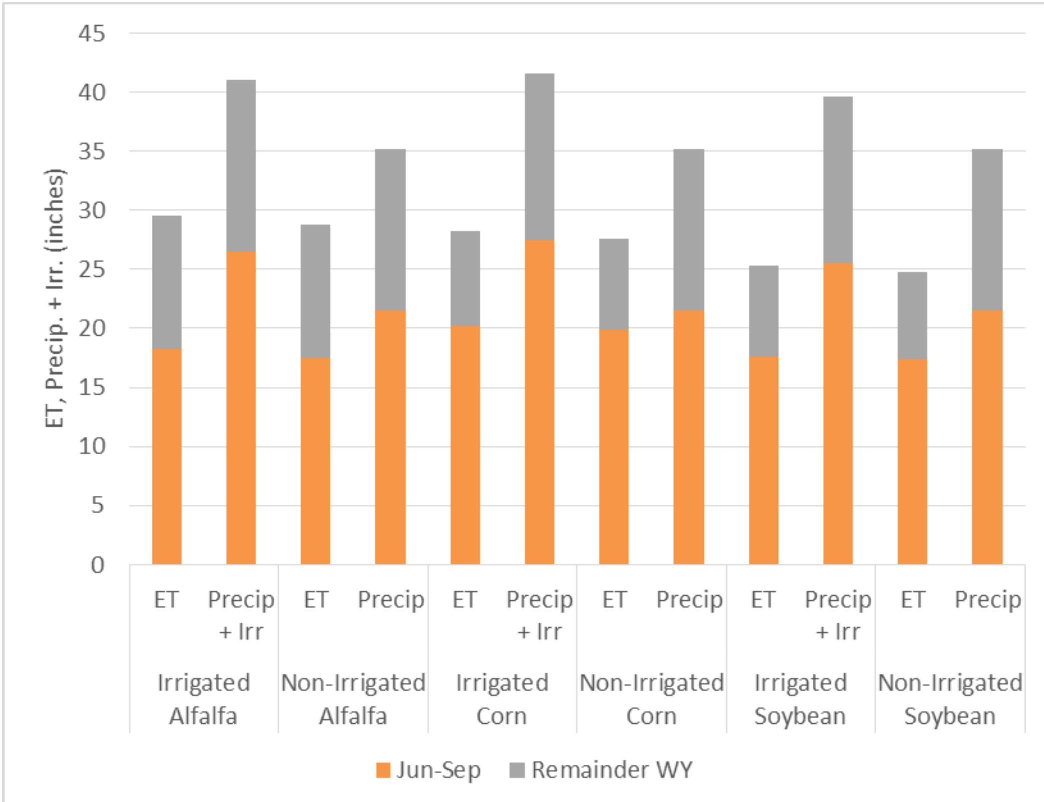

Figure F18 ET computed by the SWAT model for water year 2016.

It is possible that water stress for the non-irrigated runs was somewhat under-represented in the model, particularly in 2016. SWAT assumes a higher concentration of roots and corresponding water uptake near the surface. The default transpiration settings allow plants to extract water from deeper soil layers within the active root zone as shallower layers dry out, however. Limiting the transpiring capacity within the deeper soil layers would reduce computed ET without irrigation during some periods.

Computed annual total ET for the irrigated crops was from 20.4 to 23.6 inches in 2015 and from 26.2 to 30.5 inches in 2016. ET for alfalfa was highest followed by corn and soybeans. The average annual alfalfa ET for 2015 and 2016 was 27.0 inches compared to the average annual ET for corn-soybeans of 24.5 inches. The annual totals are generally consistent with the WEPP model results for 2005 through 2014 (Appendix A). The June through September totals were about 60 percent of the annual totals for alfalfa but about 70 percent of the annual totals for corn and soybeans. Annual total ET averaged about 10 percent more for alfalfa compared to corn and soybeans.

The differences in ET between irrigated and non-irrigated scenarios computed by SWAT for 2015 and 2016 were less than the average computed by WEPP for the 2004 through 2014 period. Water year precipitation totals applied in the SWAT model were 29.2 and 35.2 inches in 2015 and 2016 respectively. As discussed above, water stress was relatively low in 2015 and 2016, whereas the 2005 through 2014 period included years with greater water stress.

Discussion

Comparison with Reported Measurements

Seasonal ET totals from irrigated corn reported in Dylla et al. (1980) provide data to compare against modeled values. Although approximately 50 miles apart, evaporative demand is generally similar at the Westport field site to the Rice Ag Weather Network station. For example, the tall reference PET (ET_{rs}) for the Rice and Westport Ag Weather Network stations for 2015 and 2016 differed by less than 10 percent. Weather conditions at Westport in 1975 through 1978 likely differed from conditions at Rice in 2015 and 2016. Without all the necessary meteorological data, it is not possible to use the ET models to compute ET at Westport from 1975 through 1978 for direct comparison with the measurement-based values. The Dylla et al. (1980) data, nevertheless, provide relevant field data to compare against model-calculated ET for the corn growing season. Dylla et al. (1980) did not report precipitation and irrigation amounts, but sufficient water was provided such that water availability was not limiting.

The seasonal (emergence to maturity) water use, averaged among all of the lysimeters, was 24.0 and 23.7 inches in 1975 and 1976 respectively versus 17.2 and 18.3 inches in 1977 and 1978 (Figure 4). Disease and storm damage had a more severe impact on crop yields in 1977 and 1978 and, presumably, on ET. The authors note that sprinkler irrigation likely resulted in greater evaporative losses in 1975 relative to drip irrigation, but all of those additional losses were not included in the calculation of crop water use. Sprinkler irrigation amounts were measured in four catch cans surrounding each lysimeter, and water not reaching the cans was not included in the water balance calculations.

Dylla et al. (1980) compared measured ET to pan evaporation and ET calculated using both a modified form of the Jensen-Haise equation (Follett et al., 1973) and the standard version (Jensen and Haise, 1963) with crop coefficients developed for Southeastern North Dakota. The Jensen-Haise (J-H) equation uses daily solar radiation and average temperature but not wind and humidity. The J-H based ET values were substantially lower than measured ET for 1975 and 1976 (15.3 to 17.7 inches) but were closer to measured ET during the two years with more severe crop damage (1977 and 1978). Measured ET at Westport in 1975 and 1976 was higher than ET calculated using crop coefficients and the SWAT model for 2015 and 2016, but measured ET at Westport in 1977 and 1978 was lower than all but one of the modeled ET totals for 2015 and 2016.

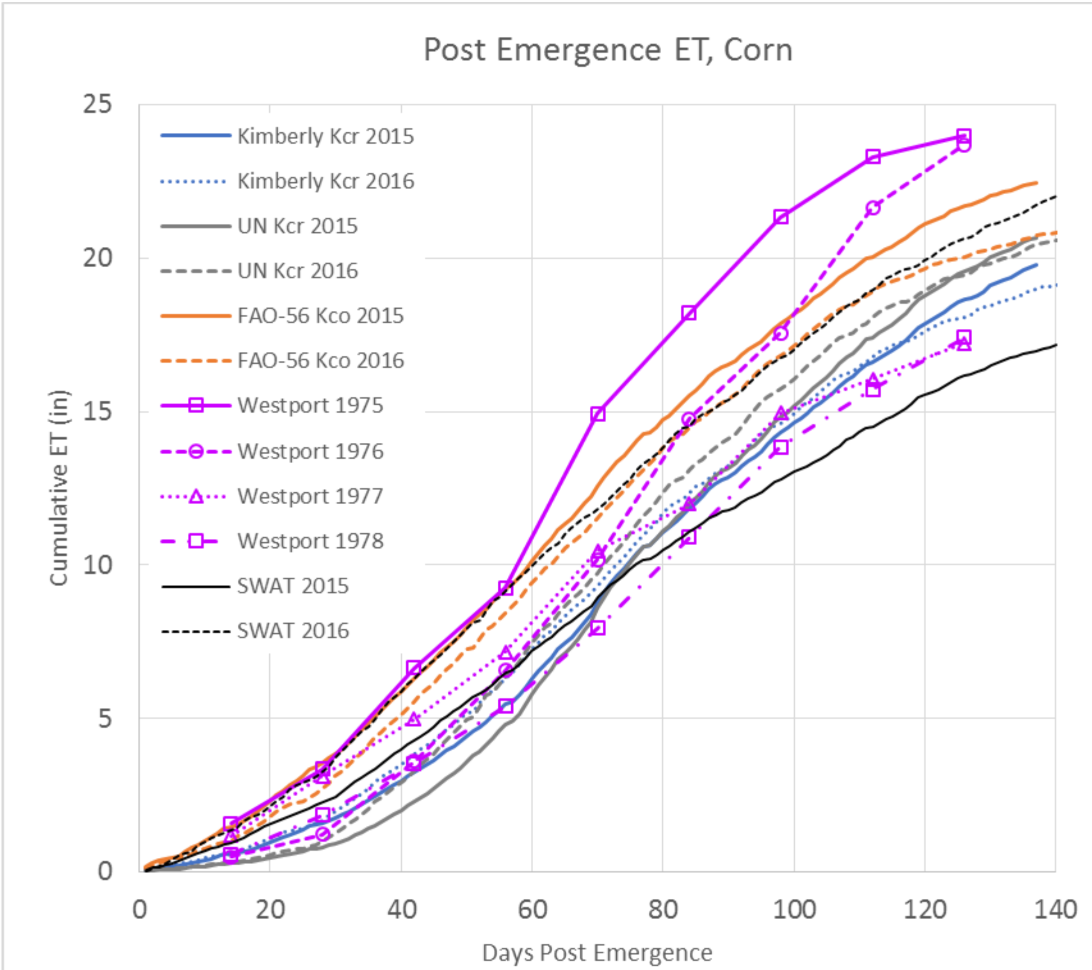

Figure F19 Calculated post-emergence ET from corn for 2015 and 2016 compared to field measurements at Westport in 1975 through 1978

The growing season (planting to harvest) ET from irrigated corn measured by Suyker and Verma (2009) from 2001 through 2005 varied from 19.8 to 22.2 inches and averaged 21.4 inches. These data cover a longer season than the Dylla et al. (1980) measurements from emergence to maturity, but they are similar. Planting to harvest ET totals computed by the SWAT model were 19.5 and 23.9 inches for 2015 and 2016 respectively.

Annual (planting to planting) ET reported by Suyker and Verma (2009) for irrigated corn varied from 24.3 to 27.7 inches and averaged 26.6 inches. Water year totals computed by the SWAT model were 22.3 and 28.3 inches for 2015 and 2016 respectively. Non-growing season ET in Eastern Nebraska is expected to typically be higher due to a longer period above freezing temperatures.

The growing season (planting to harvest) ET totals from irrigated soybeans measured by Suyker and Verma (2009) were 18.7 and 16.9 inches in 2002 and 2004, respectively. The growing season totals computed by the SWAT model for 2015 and 2016 were 16.0 and 19.8 inches. Annual totals for the eastern Nebraska measurements were 22.3 and 25.1 inches in 2002 and 2004. The water-year totals computed by the SWAT model for 2015 and 2016 were 20.3 and 25.3 inches respectively.

Average ET from the Watershed Water Budget

Longer-term, average ET is commonly estimated using a simple water-budget analysis. The water budget for a watershed can be summarized as

$P - ET - RO + U = \Delta S$

where:

P is average precipitation;
ET is average evapotranspiration;
RO is average streamflow at the watershed outlet/gauge;
U is net groundwater underflow across the topographic watershed divide; and
ΔS is change in stored water (surface, soil, and groundwater)

If the U term can be assumed to be negligible, ET is estimated as P – RO for a time period over which ΔS can be assumed to be very small relative to the cumulative values of the other terms. For watersheds such as Little Rock Creek with multiple aquifers and areas of low-topographic relief, the U term may not be negligible. Above the long-term stream gage, 15029001 (See Figure 3) the groundwater drainage area is likely very close in size to the topographic watershed area, and U will be approximated as zero. One approach to minimize ΔS is to demark "inter-drought" periods based on low base flow (Tomer and Burkart, 2003 and Tomer and Schilling, 2009).

The 15029001 gage has a nearly continuous record of streamflow starting from December 2007. Base flow was relatively low in December of 2007 following a drought year (6.0 cfs), and base flow was low in November of 2012 (5.7 cfs) following dry conditions from August through the autumn. A brief period of missing streamflow data in March and April 2012 was estimated using computed flows from the GSSHA model.

The Minnesota State Climatology Office has interpolated monthly precipitation totals from the HIDEN network of gages to a 10 kilometer grid. The average precipitation over this period for a grid point near the center of the watershed was 29.74 inches/year. The average streamflow from December 2007 through November 2012 was 22.5 cubic feet per second (cfs) or 7.15 inches/year over the 42.8 square-mile watershed. Using these values for P and RO, the average ET is estimated to be 22.6 inches/year during this period.

The estimated ET represents a spatial average for the entire watershed that includes a range of land uses with about 75 percent of the area in agricultural uses (cultivated crops, hay, and pasture). Because the estimated watershed average includes ET from wetlands and riparian areas, average ET from upland areas is expected to be less than the estimated watershed average. Also, note that the estimate is affected by measurement errors in precipitation and streamflow as well as the simplifying assumptions of the method.

The calculated watershed average ET is within the range computed by the SWAT model for irrigated and non-irrigated row crops and alfalfa for 2015 (20.1 to 23.8 inches) but is lower than the SWAT computed values for 2016 (24.8 to 29.5 inches). The average ET for water years 2005 through 2014 computed by the WEPP model varied from 19.5 inches/year (non-irrigated corn-soybean in loamy sand) to 30.9

inches/year (irrigated alfalfa in loam). The average computed ET for the entire GSSHA model domain for water years 2008 through 2012 was 25.0 inches/year. The 15029001 watershed is just under 15 percent of the GSSHA model domain, but ET for a sub-area of the model is not provided in the GSSHA model output.

Annual and Non-Irrigated ET

The single-crop coefficient methods are most uncertain during periods when crops are in the early stages of growth and after the peak growth period. Crop coefficient methods should not be applied during the non-growing season. Therefore, long-term, continuous water balances needed for multi-year hydrologic modeling require other methods. The crop-coefficient methods applied in this report also cannot be used if plants are short of water. ET under non-irrigated conditions is more dependent on soil properties and on precipitation amounts and timing.

The SWAT computed ET for alfalfa was less than corn and about the same as soybean for June through September, but annual total ET was greatest for alfalfa. This is consistent with the WEPP results (See Appendix A). This is expected because alfalfa has a longer growing season than annual crops such as corn and soybeans.

Alfalfa has a long tap root, and established alfalfa can draw water from greater soil depths than soybeans and corn (e.g., Arnold et al., 2012). Greater rooting depth allows for access to a larger reservoir of stored soil water during periods in which shallower soil layers dry out. This allows for greater ET for deeper-rooted plants under dry conditions. Alfalfa will go dormant under drought conditions and can recover when water becomes available again except under severe drought conditions (Shewmaker et al., 2013). Water stress may have more severe effects on growth and development of annual crops. Water stress is an important factor when evaluating ET under non-irrigated conditions.

Opportunities

Ongoing research will provide additional data and analysis results on ET and soil-water balance from Central Minnesota to compare against. Researchers at the University of Minnesota under the direction of Dr. David Mulla recently developed models of cropping systems under a research contract with the MDA (Jeppe Kjaersgaard, pers. comm.). The Westport Ag Weather Station is located at one of the field sites included in this research. Soil-water balance and ET are essential components of the models.

This modeling analysis will provide additional information on crop water use and soil-water balance in central Minnesota. These results can be compared with analysis for the LRCA and may provide information and insights that can be used to enhance the LRCA model in the future.

References

Abendroth, L.J., Elmore, R.W., Boyer, M.J., and Marlay, S.K., Corn Growth and Development, PMR 1009: Iowa State University Extension, Ames, Iowa, 49 p.

Akyuz, F.A., Kandel, H., and Morlock, D., 2017, Developing a growing degree day model for North Dakota and Northern Minnesota soybean: Agricultural and Forest Meteorology, Volume 239, pp. 134-140, ISSN 0168-1923, https://doi.org/10.1016/j.agrformet.2017.02.027.

Allen, R.G., Pereira, .S., Raes, D., and Smith, M., 1998, Crop evapotranspiration - Guidelines for computing crop water requirements - FAO Irrigation and drainage paper 56: Food and Agriculture Organization of the United Nations, Rome. http://www.fao.org/docrep/X0490E/X0490E00.htm

Allen, R.G. and J.L. Wright, Conversion of Wright (1981) and Wright (1982) alfalfa-based crop coefficients for use with the ASCE Standardized Penman-Monteith Reference Evapotranspiration Equation: Unpublished report, 38 p. http://www.kimberly.uidaho.edu/water/asceewri/Conversion_of_Wright_Kcs_2c.pdf

Arnold, J.G., Kiniry, J.R., Srinivasan, R., Williams, J.R., Haney, E.B., and Neitsch, S.L., 2012, Soil and Water Assessment Tool Input/Output Documentation Version 2012: Texas Water Resources Institute Report TR-439, 654 p.

Arnold, J.G., Moriasi, D.N.; Gassman, P.W., Abbaspour, K.C., White, M.J., Srinivasan, R., Santhi, C., Harmel, D., van Griensven, A., Van Liew, M.W., Kannan, N., and Jha, M.K., 2012, SWAT - Model use, calibration, and validation: Transactions of the ASABE 55(4): 1491-1508.

ASCE – EWRI, 2005, The ASCE standardized reference evapotranspiration equation, report of the Task Committee on Standardization of Reference Evapotranspiration: Environmental and Water Resources Institute of the American Society of Civil Engineers, 216 p.

Ball, J. T., Woodrow, I. E., and Berry, J. A., 1987, A model predicting stomatal conductance and its contribution to the control of photosynthesis under different environmental conditions: in Progress in Photosynthesis Research - Proceedings of the Seventh International Congress on Photosynthesis, edited by: Biggins, J., Martinus-Nijhoff Publishers, Dordrecht, The Netherlands, 221– 224, 1987.

Baratta, V.M., 2019, Groundwater Atlas of Morrison County, Minnesota: Minnesota Department of Natural Resources, County Atlas Series C-31, Part B.

Ding R, Kang S, Du T, Hao X, Zhang Y, 2014, Scaling Up Stomatal Conductance from Leaf to Canopy Using a Dual-Leaf Model for Estimating Crop Evapotranspiration: PLoS ONE 9(4): e95584. doi:10.1371/journal.pone.0095584

Dylla, A.S., Timmons, D.R., and Shull, H., 1980, Estimating water used by irrigated corn in West Central Minnesota: Soil Science Society of America Journal, 44(4), pp. 823-827.

Follet, R.F., Reichman, E.J., Doering, E.J., and Benz, L.C., 1973, A nomograph for estimating evapotranspiration: J. Soil Water Conserv. 28(2): 90-92.

Fuka, D.R., C.A. MacAllister, A.T. Degaetano, and Z.M. Easton, 2013, Using the Climate Forecast System Reanalysis dataset to improve weather input data for watershed models: Hydrol. Proc. DOI: 10.1002/hyp.10073.

Hicks, D.R., 2004, Growing degree days – corn growth and yield: Minnesota Crop News July 27, 2004. http://blog-crop-news.extension.umn.edu/2004/07/growing-degree-days-corn-growth-and.html

Jarvis, P.G., 1976, The interpretation of the variations in leaf water potential and stomatal conductance found in canopies in the field: Philosophical Transactions of the Royal Society of London. Series B, Biological Sciences 273: 593–610.

Jensen, M.E. and H.R. Haise, 1963, Estimating evapotranspiration from solar radiation: J Irrig Drain Div 89: 15-41.

Neitsch, J.G., Arnold, J.R., Kiniry, J.R., and Williams, J.R., 2011, Soil and Water Assessment Tool Theoretical Documentation Version 2009: Texas Water Resources Institute Technical Report No. 406, 618 p.

Noland, R., Holen, D., Sheaffer, C., and Wells, M.S., 2015, Alfalfa assessment – Factors leading to winter injury: University of Minnesota Extension. https://www.extension.umn.edu/agriculture/forages/growth-and-development/alfalfa-assessment/

North Central IPM Center, 2000, Crop profile for alfalfa in Minnesota: North Central Integrated Pest Management Center, University of Illinois, Urbana-Champaign. https://ipmdata.ipmcenters.org/documents/cropprofiles/mnalfalfa.pdf

Monteith, J.L., 1965, Evaporation and the environment: In The state and movement of water in living organisms, p. 205-234, XIXth Symposium. Soc. for Exp. Biol., Swansea, Cambridge Univ. Press.

Sengupta, M.; Weekley, A.; Habte, A.; Lopez, A.; Molling, C.; Heidinger, A., 2015, Validation of the National Solar Radiation Database (NSRDB) (2005–2012): Preprint, 6 pp. NREL/CP-5D00-64981.

Sengupta, M.; Habte, A.; Gotseff, P.; Weekley, A.; Lopez, A.; Molling, C.; Heidinger, A., 2014, Physics-based GOES satellite product for use in NREL's National Solar Radiation Database: Preprint, 9 p. NREL/CP-5D00-62237.

Shewmaker, G.E., Allen, R.G., and Neibling, W.H., 2013, Alfalfa irrigation and drought: University of Idaho Extension Fact Sheet, 7 p.

Stewart, J.B., 1988, Modelling surface conductance of pine forest: Agric. For. Meteorol. 43, 19-3

Suyker, AE and Verma, S, 2009, Evapotranspiration of irrigated and rainfed maize–soybean cropping systems: Agricultural and Forest Meteorology 149 (3-4), 443–452.

Tomer, M.D. and Burkart, M.R., 2003, Long term effects of nitrogen fertilizer use on ground water nitrate in two small watersheds: J. Environ. Qual. 32 (6), 2158–2171.

Tomer, MD and Schilling, KE, 2009, A simple approach to distinguish land-use and climate-change effects on watershed hydrology: Journal of Hydrology 376, 24-33.

USDA-NRCS, 1997, National Engineering Handbook – Part 630 Hydrology: U.S. Department of Agriculture, Natural Resource Conservation Service.

USDA-NRCS, Official Soil Series Descriptions: U.S. Department of Agriculture, Natural Resource Conservation Service., https://www.nrcs.usda.gov/wps/portal/nrcs/detailfull/soils/survey/class/data/?cid=nrcs142p2_053587.

University of Minnesota Extension, 1999, Minnesota soybean field book: Bennett, J.M., Hicks, D.R., and Naeve, S.L. eds., 157 p.